Investigation of Organolanthanide-Based Carbon–Carbon Bond Formation: Synthesis, Structure, and Coupling Reactivity of Organolanthanide Alkynide Complexes, Including the Unusual Structures of the Trienediyl Complex $[(C_5Me_5)_2Sm]_2[\mu\text{-}\eta^2\text{:}\eta^2\text{-}Ph(CH_2)_2C{=}C{=}C{=}C\text{-}(CH_2)_2Ph]$ and the Unsolvated Alkynide $[(C_5Me_5)_2Sm(C{\equiv}CCMe_3)]_2$[1]

William J. Evans,* Roy A. Keyer, and Joseph W. Ziller

Department of Chemistry, University of California, Irvine, Irvine, California 92717

Received April 1, 1993

The C–C bond formation which occurs when two $[PhC{\equiv}C]^-$ ligands on Cp^*_2Sm-containing organosamarium complexes are coupled to form the $[PhC{=}C{=}C{=}CPh]^{2-}$ trienediyl ligand in $[Cp^*_2Sm]_2(\mu\text{-}\eta^2\text{:}\eta^2\text{-}PhC{=}C{=}C{=}CPh)$ (**1**) has been investigated ($Cp^* = C_5(CH_3)_5$). The generality of the reactions which form **1**, namely the reactions of $[Cp^*_2Sm(\mu\text{-}H)]_2$ and Cp^*_2Sm with $HC{\equiv}CPh$ and the thermolysis of $Cp^*_2Sm(C{\equiv}CPh)(THF)$ (**2**), has been probed by examining the reactivity of a variety of lanthanide alkynide systems. The bis(alkynide) complexes $[Cp^*_2Ln(\mu\text{-}C{\equiv}CPh)_2K]_n$ (Ln = Ce (**3**), Nd (**4**), Sm (**5**)) do not undergo the coupling reaction, but trienediyl complexes have been obtained by heating $Cp^*_2Ce(C{\equiv}CPh)(THF)$ (**9**) and $Cp^*_2Nd(C{\equiv}CPh)(THF)$ (**10**), which demonstrates that a readily accessible divalent state is not a requirement for the coupling. **9** and **10** are conveniently made from $Cp^*_2Ln[N(SiMe)_2]$ and $PhC{\equiv}CH$ in a metathesis reaction which succeeds in THF but unexpectedly fails in toluene. Coupled trienediyl products $[Cp^*_2Sm]_2[\mu\text{-}\eta^2\text{:}\eta^2\text{-}Ph(CH_2)_2C{=}C{=}C{=}C(CH_2)_2Ph]$ (**19**) and $[Cp^*_2Sm]_2[\mu\text{-}\eta^2\text{:}\eta^2\text{-}Me_2CH(CH_2)_2C{=}C{=}C{=}C(CH_2)_2CHMe_2]$ (**20**) have also been obtained from the reaction of Cp^*_2Sm with $HC{\equiv}C(CH_2)_2Ph$ and $HC{\equiv}C(CH_2)_2CHMe_2$, respectively. The NMR spectra and X-ray crystal structures of these products show agostic interactions involving methylene groups. The reaction of $[Cp^*_2Sm(\mu\text{-}H)]_2$ with $HC{\equiv}CCMe_3$ generates the loosely joined dimeric alkynide $[Cp^*_2Sm(C{\equiv}CCMe_3)]_2$ (**17**) and the unusual insertion product $Cp^*_2Sm[Me_3CCH{=}CC(CMe_3){=}CH_2]$ (**18**). The steric and electronic factors responsible for the observed chemistry are discussed, as well as a samarium-based cycle involving trienediyl **1** for the formation of enynes from alkynes. X-ray crystallography was used to definitively identify several of the products and synthetic precursors. $[Cp^*_2Sm(\mu\text{-}C{\equiv}CPh)_2K]_n$ (**5**) crystallizes in space group $P2_12_12_1$ with $a = 9.8590(15)$ Å, $b = 16.251(3)$ Å, $c = 20.242(4)$ Å, $V = 3243(1)$ Å^3, and $D_{calcd} = 1.356$ g cm^{-3} for $Z = 4$. Least-squares refinement of the model based on 3110 reflections converged to a final $R_F = 2.6\%$. In **5**, the two Cp* ring centroids and the two alkynide α-carbon atoms define a distorted tetrahedron around samarium. The potassium atom is bound to both alkynide ligands of one molecular unit and to a Cp* ligand of the adjacent molecule to generate a polymeric species. $Cp^*_2Sm[N(SiMe_3)_2]$ (**8**) crystallizes from toluene in space group $R\bar{3}$ with $a = 17.695(2)$ Å, $c = 47.269(5)$ Å, $V = 12\,818(2)$ Å^3, and $D_{calcd} = 1.355$ g cm^{-1} for $Z = 18$. Least-squares refinement of the model based on 4940 reflections converged to a final $R_F = 4.1\%$. The amide ligand in **8** is attached symmetrically to the Cp^*_2Sm unit such that the two ring centroids, the amide nitrogen, and the samarium are coplanar to within 0.05 Å. $[Cp^*_2Sm(C{\equiv}CCMe_3)]_2$ (**17**) crystallizes from toluene in space group *Pbca* with $a = 14.753(2)$ Å, $b = 17.682(3)$ Å, $c = 22.966(4)$ Å, $V = 5991(2)$ Å^3, and $D_{calcd} = 1.297$ g cm^{-1} for $Z = 8$. Least-squares refinement of the model based on 2917 reflections converged to a final $R_F = 7.3\%$. Each alkynide ligand in a monomeric unit of **17** is attached asymmetrically to the Cp^*_2Sm unit such that samarium lies 0.38 Å out of the plane defined by the two Cp* ring centroids and the alkynide α-carbon atoms. A methyl group from the Cp* ligand of another monomer is oriented toward samarium at a distance of 3.006(7) Å to generate a loosely linked dimeric structure. $Cp^*_2Sm[Me_3CCH{=}CC(CMe_3){=}CH_2]$ (**18**) crystallizes from toluene in space group *Pbca* with $a = 14.753(2)$ Å, $b = 17.682(3)$ Å, $c = 22.966(4)$ Å, $V = 5991(2)$ Å^3, and $D_{calcd} = 1.297$ g cm^{-3} for $Z = 8$. Least-squares refinement of the model based on 2917 reflections converged to a final $R_F = 6.0\%$. In **18**, a 1,3-di-*tert*-butyl-1,3-butadien-2-yl ligand is attached to Cp^*_2Sm via a 2.484(14) Å Sm–C bond. $[Cp^*_2Sm]_2[\mu\text{-}\eta^2\text{:}\eta^2\text{-}Ph(CH_2)_2C{=}C{=}C{=}C(CH_2)_2Ph]$ (**19**) crystallizes from toluene in space group $C2/c$ with $a = 28.589(6)$ Å, $b = 10.5209(16)$ Å, $c = 22.450(3)$ Å, $\beta = 110.924(14)°$, $V = 6307(2)$ Å^3, and $D_{calcd} = 1.352$ g cm^{-3} for $Z = 4$. Least-squares refinement of the model based on 4655 reflections converged to a final $R_F = 5.3\%$. In **19**, the eight-carbon chain of the trienediyl and the two samarium atoms are coplanar to within 0.09 Å. The two shortest Sm–C distances connecting a Cp^*_2Sm unit to the ligand are 2.483(7) and 2.689(6) Å. A methylene group is oriented toward each Cp^*_2Sm unit at a distance of 3.748 Å.

Introduction

Carbon–carbon bond-forming reactions are of fundamental importance in organometallic chemistry.[2] Reductive elimination (eq 1) is one of the several ways in which transition metals can form C–C bonds, but it is not considered to be a viable reaction pathway for lanthanide metal complexes,[3] because no lanthanide has the necessary

(1) Reported in part at the 203rd National Meeting of the American Chemical Society, San Francisco, CA, April 1992; INOR 671.

(2) Collman, J. P.; Hegedus, L. S.; Norton, J. R.; Finke, R. G. *Principles and Applications of Organotransition Metal Chemistry*; University Science Books: Mill Valley, CA, 1987. (b) Yamamoto, A. *Organotransition Metal Chemistry*; Wiley: New York, NY, 1986.

0276-7333/93/2312-2618$04.00/0

two-electron redox couple.[4] Bimetallic reductive eliminations[5] are conceivable for organolanthanide complexes and may even be thermodynamically favored,[6] but they have never been observed. Given the traditional view that

$$L_xM\begin{matrix}R\\R'\end{matrix} \longrightarrow L_xM + R{-}R' \qquad (1)$$

lanthanide complexes have considerable ionic character and that Ln–C bonds are rather polarized with negative charge on the carbon atom, the formation of a C–C bond by reductive elimination of two organlanthanide ligands would be expected to be electrostatically disfavored. Hence, polyalkyl complexes such as $(LnMe_6)^{3-}$,[7] $[LnR_4]^-$,[8] $[Ln(C{\equiv}CR)_4]^-$,[9] LnR_3Cl^-,[10] $[(C_5Me_5)LnR_3]^-$,[11] LnR_3,[12] and $(C_5R_5)LnR_2$[13] can be isolated and show no evidence of C–C bond-forming reactivity between the ligands.

Therefore, it was of considerable interest when it was discovered that a C–C bond formation reaction could be accomplished using alkynide ligands on lanthanide metal centers[14] as shown in eqs 2–5 (Cp* = C_5Me_5). This was

$$2Cp^*_2Sm[CH(SiMe_3)_2] + 2PhC{\equiv}CH \longrightarrow 1 \qquad (2)$$

$$[Cp^*_2Sm(\mu\text{-}H)]_2 + 2PhC{\equiv}CH \longrightarrow 1 \qquad (3)$$

$$2Cp^*_2Sm + 2PhC{\equiv}CH \longrightarrow 1 \qquad (4)$$

$$2Cp^*_2Sm(C{\equiv}CPh)(THF) \longrightarrow 1 \qquad (5)$$

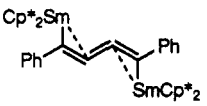

$[Cp^*_2Sm]_2[\mu\text{-}\eta^2{:}\eta^2\text{-}PhC{=}C{=}C{=}CPh]$ (1)

the first example in lanthanide or actinide chemistry in which two formally anionic ligands coupled to form a C–C bond. Moreover, the reaction appeared to be particularly facile: not only could it be accomplished at low temperature, but its existence was not detected in a thermodynamic study[6] of organosamarium complexes, which assumed that "$[Cp^*_2Sm(\mu\text{-}C{\equiv}CPh)]_2$" was the product of eq 2.

The coupling of alkynes to diynes has been known for decades, and these reactions are commonly thought to occur via radical pathways.[15] Although a radical mechanism for eqs 2–5, as shown in eqs 6–8, contains two well-precedented steps, eqs 7[15] and 8,[16] it also requires several difficult transformations. These include the homolytic cleavage of a strong Sm–alkynide bond[17] (eq 6), the formation of strongly reducing Sm(II) from Sm(III)[4] (eq 6), and a selective combination of the radicals present. Interestingly, facile Sm(III) to Sm(II) reductions have been observed[22-24] (eqs 9–12). In addition, such a radical coupling pathway has been discussed for a Ti^{III}—C≡CPh

$$2"Cp^*_2Sm{-}C{\equiv}CPh" \rightarrow 2Cp^*_2Sm + 2{\cdot}C{\equiv}CPh \qquad (6)$$

$$2{\cdot}C{\equiv}CPh \rightarrow PhC{\equiv}CC{\equiv}CPh \qquad (7)$$

$$2Cp^*_2Sm + PhC{\equiv}CC{\equiv}CPh \rightarrow (Cp^*_2Sm)_2(\mu\text{-}\eta^2{:}\eta^2\text{-}PhC{=}C{=}C{=}CPh) \qquad (8)$$

$$2(Cp^*_2Sm)_2(PhC_2Ph) + 4THF \rightarrow 2Cp^*_2Sm(THF)_2 + 2PhC{\equiv}CPh \qquad (9)[22]$$

$$(Cp^*_2Sm)_2(\mu\text{-}\eta^2{:}\eta^3\text{-}PhCHCH_2) + 4THF \rightarrow 2Cp^*_2Sm(THF)_2 + PhCH{=}CH_2 \qquad (10)[23]$$

$$(Cp^*_2Sm)_2(\mu\text{-}\eta^2{:}\eta^4\text{-}PhCHCHPh) + 4THF \rightarrow 2Cp^*_2Sm(THF)_2 + PhCH{=}CHPh \qquad (11)[23]$$

$$(Cp^*_2Sm)_2(\mu\text{-}\eta^2{:}\eta^2\text{-}N_2) + 2THF \rightarrow 2Cp^*_2Sm(THF)_2 + N_2 \qquad (12)[24]$$

system which forms a related $(PhCCCCPh)^{4-}$ product.[14,25]

Since the alkynide coupling reactions 2–5 constituted the first reported organo-f-element C–C bond formation

(3) (a) Marks, T. J.; Ernst, R. D. In *Comprehensive Organometallic Chemistry*; Wilkinson, G., Stone, F. G. A., Abel, E. W., Eds.; Pergamon Press: Oxford, England, 1982; Chapter 21. (b) Schumann, H.; Genthe, W. In *Handbook on the Physics and Chemistry of Rare Earths*; Gschneidner, K. A., Jr., Eyring, L., Eds.; Elsevier: Amsterdam, 1985; Vol. 7, Chapter 53 and references therein. (c) Forsberg, J. H.; Moeller, T. In *Gmelin Handbook of Inorganic Chemistry*, 8th ed.; Moeller, T., Kruerke, U., Schleitzer-Rust, E., Eds.; Springer-Verlag: Berlin, 1983; Part D6, pp 137–282. (d) Evans, W. J. *Adv. Organomet. Chem.* **1985**, *24*, 131–177.

(4) Morss, L. R. *Chem. Rev.* **1976**, *76*, 827–841.

(5) Halpern, J. *Inorg. Chim. Acta* **1982**, *62*, 31–37. Hoffmann, R.; Trinquier, G. *Organometallics* **1984**, *3*, 370–380.

(6) Nolan, S. P.; Stern, D.; Marks, T. J. *J. Am. Chem. Soc.* **1989**, *111*, 7844–7853.

(7) Schumann, H.; Muller, J.; Bruncks, N.; Lauke, H.; Pickardt, J.; Schwarz, H.; Eckart, K. *Organometallics* **1984**, *3*, 69–74.

(8) Wayda, A. L.; Evans, W. J. *J. Am. Chem. Soc.* **1978**, *100*, 7119–7121. Schumann, H.; Muller, J. *J. Organomet. Chem.* **1979**, *169*, C1-C4. Schumann, H.; Genthe, W.; Hahn, E.; Pickardt, J.; Schwarz, H.; Eckart, K. *J. Organomet. Chem.* **1986**, *306*, 215–225. Hitchcock, P. B.; Lappert, M. F.; Smith, R. G. *J. Chem. Soc., Chem. Commun.* **1989**, 369–371.

(9) Evans, W. J.; Wayda, A. L. *J. Organomet. Chem.* **1980**, *202*, C6–C8.

(10) Atwood, J. L.; Lappert, M. F.; Smith, R. G.; Zhang, H. *J. Chem. Soc., Chem. Commun.* **1988**, 1308–1309. Atwood, J. L.; Hunter, W. E.; Rogers, R. D.; Holton, J.; McMeeking, J.; Pearce, R.; Lappert, M. F. *J. Chem. Soc., Chem. Commun.* **1978**, 140–142. Schaverien, C. J.; van Mechelen, J. B. *Organometallics* **1991**, *10*, 1704–1709.

(11) Schumann, H.; Albrecht, I.; Pickardt, J.; Hahn, E. *J. Organomet. Chem.* **1984**, *276*, C5–C9.

(12) Hitchcock, P. B.; Lappert, M. F.; Smith, R. G.; Bartlett, R. A.; Power, P. P. *J. Chem. Soc., Chem. Commun.* **1988**, 1007–1009.

(13) (a) Heeres, H. J.; Meetsma, A.; Teuben, J. H.; Rogers, R. D. *Organometallics* **1989**, *8*, 2637–2646. (b) van der Heiden, H.; Schaverien, C. J.; Orpen, A. G. *Organometallics* **1989**, *8*, 255–258.

(14) Evans, W. J.; Keyer, R. A.; Ziller, J. W. *Organometallics* **1990**, *9*, 2628–2631.

(15) (a) Glaser, C. *Ber. Dtsch. Chem. Ges.* **1869**, *2*, 422. (b) Cadiot, P.; Chodkiewicz, W. In *The Chemistry of Acetylenes*; Viehe, G. H., Eds.; Marcel Dekker: New York, 1969; Chapter 9. (c) Shostakovski, M. F.; Bogdanova, A. V. In *The Chemistry of Diacetylenes*; Wiley: New York, 1974. (d) Eglinton, G.; McCrae, W. *Adv. Org. Chem.* **1963**, *4*, 225–328. (e) Gotzig, J.; Otto, H.; Werner, H. *J. Organomet. Chem.* **1985**, *287*, 247.

(16) Evans, W. J.; Keyer, R. A.; Zhang, H.; Atwood, J. L. *J. Chem. Soc., Chem. Commun.* **1987**, 837–838.

(17) Although the strength of a Sm—CCR bond is not known from the study in ref 6, it is likely that this bond is strong, on the basis of the known metal–alkynide bond strengths[18] and correlation between Sm—Z and H—Z bonds.[18-21]

(18) Bryndza, H. E.; Fong, L. K.; Paciello, R. A.; Tam, W.; Bercaw, J. E. *J. Am. Chem. Soc.* **1987**, *109*, 1444–1456.

(19) Nolan, S. P.; Porchia, M.; Marks, T. J. *Organometallics* **1991**, *10*, 1450–1457.

(20) Nolan, S. P.; Stern, D.; Hedden, D.; Marks, T. J. *ACS Symp. Ser.* **1990**, *No. 428*, 159–174.

(21) Marks, T. J.; Gagne, M. R.; Nolan, S. P.; Schock, L. E.; Seyam, A. M.; Stern, D. *Pure Appl. Chem.* **1989**, *61*, 1665–1672.

(22) Evans, W. J.; Bloom, I.; Hunter, W. E.; Atwood, J. L. *J. Am. Chem. Soc.* **1983**, *105*, 1401–1403.

(23) Evans, W. J.; Ulibarri, T. A.; Ziller, J. W. *J. Am. Chem. Soc.* **1990**, *112*, 219–223.

(24) Evans, W. J.; Ulibarri, T. A.; Ziller, J. W. *J. Am. Chem. Soc.* **1988**, *110*, 6877–6879.

(25) Sekutowski, D. G.; Stucky, G. D. *J. Am. Chem. Soc.* **1976**, *98*, 1376–1382.

reaction of this type, we have expanded our study of this system to probe its generality. We report here on (a) the synthesis of a series of organolanthanide alkynide complexes, including the mono- and bis(alkynide) complexes $Cp^*_2Ln(C{\equiv}CR)(THF)$ and $[Cp^*_2Ln(C{\equiv}CR)_2]^-$, (b) the reactivity of these alkynide complexes with respect to the coupling reaction, (c) the structure and properties of the corresponding trienediyl complexes $[Cp^*_2Ln]_2(RC{=}C{=}C{=}CR)$ obtained by coupling, and (d) a samarium-based cycle involving trienediyl complexes for coupling alkynes to enynes. Both Ln and R have been varied in this study to determine the importance of an accessible divalent oxidation state and the steric and electronic effects of the alkynide substituent.

These studies on alkynide reactivity have also generated additional unexpected results in areas other than coupling reactivity. First, in order to conveniently obtain a variety of alkynide complexes, the synthetic utility of organolanthanide amides was developed and the reactivity of these complexes was found to have an unanticipated solvent dependence. Second, the surprising structure of an unsolvated dimeric *tert*-butyl alkynide complex, $[Cp^*_2Sm(C{\equiv}CCMe_3)]_2$, has been identified which suggests new opportunities to study electrophilic organolanthanide coordination chemistry. Third, a dienyl complex of unusual structure has also been identified which has interesting implications with respect to organolanthanide insertion chemistry. These points are described, as well as our results on alkynide reactivity.

Experimental Section

The compounds described below were handled under nitrogen with the rigorous exclusion of air and water using Schlenk, high-vacuum, and glovebox (Vacuum Atmospheres HE-553 Dri-Lab) techniques. Solvents were dried, and physical measurements were obtained as previously described.[26,27] PhC≡CH (Aldrich), ^{t}BuC≡CH (Aldrich), $Et_2NCH_2C{\equiv}CH$ (Farchan), $PhCH_2CH_2C{\equiv}CH$ (Farchan), $Me_2CHCH_2CH_2C{\equiv}CH$ (Farchan), and $Me_2CHC{\equiv}CH$ (Farchan) were dried over sieves, vacuum-transferred, and stored under nitrogen. KH (Aldrich) was washed with THF to remove the oil and dried under vacuum. $KN(SiMe_3)_2$ (Aldrich, 0.5 M solution in toluene) was used without further purification. $Cp^*_2Sm(THF)_x$ (x = 0–2),[28] $Cp^*_2Sm(C{\equiv}CR)(THF)$ (R = Ph, CMe_3),[26] and $[Cp^*_2Sm(\mu\text{-}H)]_2$[22] were synthesized as previously described. The complexes $Cp^*_2LnCl_2K(THF)$ (Ln = Ce, Nd, Sm) were synthesized in a manner similar to the synthesis of the lithium analogs $Cp^*_2LnCl_2Li(ether)_2$ (Ln = La, Nd, Sm, Lu)[29] with KCp* substituted for LiCp*. KC≡CPh was prepared by reacting 2 equiv of the alkyne with 1 equiv of KH in THF (the 2:1 alkyne:KH stoichiometry was found to yield a purer product). The solution was centrifuged to remove the precipitated salt; the colorless salt was washed with hexanes to remove the excess alkyne, and it was dried under vacuum. GC/MS (CI) was performed on a Finnigan spectrometer using a 50-ft DB1 column heated to 200 °C at a rate of 10 °C/min with He as a carrier gas.

$[Cp^*_2Ce(C{\equiv}CPh)_2K]_n$ (3). In a glovebox, a flask was charged with $Cp^*_2CeCl_2K(THF)$ (62 mg, 0.12 mmol), KC≡CPh (33 mg, 0.24 mmol), and 10 mL of toluene. This reaction mixture was stirred over a 24-h period and slowly turned from a bright yellow suspension to a purple solution. The reaction mixture was centrifuged to give a purple solution and a mixture of red-brown and purple solids. These solids were extracted with toluene to separate the slightly soluble purple material from the insoluble red-brown solids. All of the toluene fractions were combined, and the solvent was removed under vacuum to yield blue **3** (53 mg, 0.082 mmol, 69%). ^{1}H NMR (C_6D_6): δ 3.07 (d, J = 8 Hz, 4H, *o*-Ph), 3.72 (s, 30H, C_5Me_5), 5.16 (t, J = 8 Hz, 4H, *m*-Ph), 5.82 (t, J = 7 Hz, 2H, *p*-Ph). ^{1}H (THF-d_8): δ 2.98 (d, J = 8 Hz, 4H, *o*-Ph), 3.36 (s, 30H, Cp*), 5.32 (t, J = 8 Hz, 4H, *m*-Ph), 5.95 (t, J = 7 Hz, 2H, *p*-Ph). ^{13}C (THF-d_8): δ 9.9 (q, J = 122 Hz, C_5Me_5), 78.8 (s, C≡C), 106.0 (s, C≡C), 122.0 (d, J = 161 Hz, Ph), 123.0 (d, J = 162 Hz, Ph), 126.8 (d, J = 158 Hz, Ph), 127.6 (s, *ipso*-Ph). IR (KBr): 3026 w, 2966 w, 2959 m, 2902 s, 2865 s, 1593 w, 1495 w, 1482 s, 1440 m, 1193 m, 1068 w, 1024 w, 891 s, 771 m, 756 s, 730 s cm^{-1}. Anal. Calcd for $C_{36}H_{40}KCe$: C, 66.32; H, 6.19; Ce, 21.49; K, 6.00. Found: C, 66.06; H, 6.10; Ce, 21.20; K, 6.11. **3** was crystallized from toluene at −34 °C and found by X-ray crystallography to be have the same atomic connectivity as in complex **5**, described in full below. $[[(\mu\text{-}C_5Me_5)(C_5Me_5)Ce(\mu\text{-}C{\equiv}CPh)_2K]\cdot 0.5(toluene)]_n$ crystallizes from toluene at −34 °C in space group *Pnma* with a = 16.218(2) Å, b = 23.408(2) Å, c = 10.071(2) Å, V = 3823 Å^3, and Z = 4. Refinement of the structural data was hindered by disorder in the Cp* rings.

$[Cp^*_2Nd(C{\equiv}CPh)_2K]_n$ (4). As described above for **3**, $Cp^*_2NdCl_2K(THF)$ (212 mg, 0.390 mmol) was reacted with KC≡CPh (120 mg, 0.856 mmol) in 10 mL of toluene to form green **4** (189 mg, 0.288 mmol, 71%). ^{1}H NMR (C_6D_6): δ 2.34 (d, J = 8 Hz, 4 H, Ph), 4.55 (t, J = 7 Hz, 4H, Ph), 5.45 (t, J = 7 Hz, 2H, Ph), 7.06 (s, 30 H, Cp*). ^{1}H NMR (C_4D_8O): δ 2.01 (d, J = 7 Hz, 4H, Ph), 4.71 (t, J = 7 Hz, 4H, Ph), 5.67 (t, J = 7 Hz, 2H, Ph), 6.66 (s, 30H, Cp*). ^{13}C NMR (C_4D_8O): δ −14.1 (q, J = 122 Hz, C_5Me_5), 111.9 (d, J = 159 Hz, Ph), 120.9 (d, J = 163 Hz, Ph), 126.0 (s), 126.4 (d, J = 157 Hz, Ph), 128.9 (s), 129.7 (s), 144.5 (s). IR (thin film): 2962 s, 2906 s, 2856 s, 2725 w, 2050 w, 1967 w, 1881 w, 1594 m, 1569 w, 1481, s, 1444 m, 1375 w, 1262 m, 1194 w, 1081 m, 1068 m, 1056 m, 1025 m, 975 w, 906 w, 800 m, 768 m, 756 s, 694 s cm^{-1}. A sample for analysis was prepared as the THF solvate by dissolving **4** in THF and removing the solvent under vacuum. Anal. Calcd for $C_{40}H_{48}KONd$: C, 65.98; H, 6.64; Nd, 19.80; K, 5.37. Found: C, 62.96; H, 6.47; Nd, 20.35; K, 5.18.

$[Cp^*_2Sm(C{\equiv}CPh)_2K]_n$ (5). As described above for **3**, $Cp^*_2SmCl_2K(THF)$ (40 mg, 0.075 mmol) was reacted with KC≡CPh (21 mg, 0.15 mmol) in 10 mL of toluene to form orange **5** (32 mg, 0.048 mmol, 64%). ^{1}H NMR (C_6D_6): δ 2.01 (s, 30H, Cp*), 6.63 (d, J = 7 Hz, 4H, *m*-Ph), 6.76 (t, J = 7 Hz, 2H, *p*-Ph), 6.79 (t, J = 8 Hz, 4H, *o*-Ph). ^{1}H NMR (C_4D_8O): δ 1.72 (s, C_5Me_5), 6.52 (d, J = 8 Hz, *m*-Ph), 6.76 (t, J = 6 Hz, *p*-Ph), 6.84 (t, J = 8 Hz, *o*-Ph). ^{13}C NMR (C_4D_8O): δ 15.5 (q, J = 124 Hz, C_5Me_5), 95.1 (s, C≡C), 114.3 (s, C_5Me_5), 125.8 (s, *ipso*-Ph), 126.0 (d, J = 158 Hz, Ph), 128.0 (d, J = 157 Hz, Ph), 131.8 (d, J = 159 Hz, Ph), 138.5 (s, C≡C). IR (KBr): 2975 m, 2965 s, 2947 s, 2866 s, 2861 s, 2039 w, 1653 w, 1594 w, 1541 w, 1505 w, 1494 m, 1472 w, 1439 m, 1399 w, 1377 m, 1355 w, 1194 m, 1066 m, 1040 m, 1025 m, 772 w, 756 s, 691 m, 628 m, 605 m cm^{-1}. Anal. Calcd for $C_{36}H_{40}KSm$: C, 65.30; H, 6.04; Sm, 22.71; K, 5.90. Found: C, 65.15; H, 6.02; Sm, 22.60; K, 5.74.

X-ray Data Collection, Structure Determination, and Refinement for $[Cp^*_2Sm(C{\equiv}CPh)_2K]_n$ (5). A yellow crystal of approximate dimensions 0.23 × 0.40 × 0.40 mm was immersed in Paratone-D oil (Exxon). The oil-coated crystal was then manipulated in air onto a glass fiber and transferred to the nitrogen stream of a Siemens P3 diffractometer which is equipped with a locally modified LT-2 low-temperature system. The determination of Laue symmetry, crystal class, unit cell parameters, and the crystal's orientation matrix were carried out by previously described methods similar to those of Churchill.[30] Intensity data were collected at 173 K using a θ–2θ scan technique with Mo Kα radiation under the conditions listed in Table I.

All 3266 data were corrected for absorption and for Lorentz and polarization effects and were placed on an approximately

(26) Evans, W. J.; Ulibarri, T. A.; Chamberlain, L. R.; Ziller, J. W.; Alvarez, D. *Organometallics* **1990**, *9*, 2124–2130.
(27) Evans, W. J.; Chamberlain, L. R.; Ulibarri, T. A.; Ziller, J. W. *J. Am. Chem. Soc.* **1988**, *110*, 6423–6432.
(28) Evans, W. J.; Ulibarri, T. A. *Inorg. Synth.* **1990**, *27*, 155–157.
(29) Jeske, G.; Lauke, H.; Mauermann, H.; Swepston, P. N.; Schumann, H.; Marks, T. J. *J. Am. Chem. Soc.* **1985**, *107*, 8091–8103.
(30) Churchill, M. R.; Lashewycz, R. A.; Rotella, F. J. *Inorg. Chem.* **1977**, *16*, 265–271.

Table I. Crystal Data and Summary of Intensity Data Collection and Structure Refinement for $[(C_5Me_5)_2Sm(C{\equiv}CPh)_2K]_n$ (5), $(C_5Me_5)_2Sm[N(SiMe_3)_2]$ (8), $[(C_5Me_5)_2Sm(C{\equiv}CCMe_3)]_2$ (17), $(C_5Me_5)_2Sm[Me_3CCH{=}CC(CMe_3){=}CH_2]$ (18), and $[(C_5Me_5)_2Sm]_2[\mu\text{-}\eta^2\text{:}\eta^2\text{-}PhCH_2CH_2C{=}C{=}C{=}CCH_2CH_2Ph]$ (19)

	5	8	17	18	19
formula	$C_{36}H_{40}KSm$	$C_{26}H_{48}NSi_2Sm$	$C_{26}H_{39}Sm$	$C_{32}H_{50}Sm$	$C_{74}H_{94}Sm_2$
mol wt	662.1	581.2	501.9	585.1	1284.2
space group	$P2_12_12_1$	$R\bar{3}$	$P\bar{1}$	*Pbca*	*C2/c*
cell constants					
a, Å	9.8590(15)	17.6951(16)	9.9246(13)	14.753(2)	28.589(6)
b, Å	16.251(3)		14.459(2)	17.682(3)	10.5209(16)
c, Å	20.242(4)	47.269(5)	19.331(3)	22.966(4)	22.450(3)
α, deg			71.992(12)		
β, deg			87.933(12)		110.924(14)
γ, deg			69.859(10)		
V, Å^3	3243.0(10)	12 818(2)	2469.0(6)	75991(2)	6307(2)
Z	4	18	4	8	4
D_{calc}, g cm^{-3}	1.356	1.355	1.350	1.297	1.352
temp, K	272	183	173	183	183
radiation	MoKα; λ = 0.710 73 Å	MoKα; λ = 0.710 73 Å	MoKα; λ = 0.710 73 Å	MoKα; λ = 0.710 73 Å	MoKα; λ = 0.710 73 Å
no. of reflns collected	3266	12 051	9287	4405	6046
no. of obsd rflns with $\lvert F_o\rvert > 3.0\sigma(\lvert F_o\rvert)$	3110	4536	7384	2917	4655
transmissn coeff: min–max	0.34–0.43	0.67–0.82	0.45–0.60	0.42–0.51	0.67–0.80
R_F, %	2.61	4.1	3.7	5.98	5.31
R_{wF}, %	3.07	4.2	4.1	7.15	6.89
goodness of fit	1.23	1.52	1.83	2.05	1.94
no. of variables	345	271	488	298	338

absolute scale. The diffraction symmetry was *mmm* with systematic absences *h*00 for $h = 2n + 1$, 0*k*0 for $k = 2n + 1$, and 00*l* for $l = 2n + 1$. The space group is therefore uniquely defined as the noncentrosymmetric orthorhombic $P2_12_12_1$ (D^4_2; No. 19).

All crystallographic calculations were carried out using either the UCI-modified version of the UCLA Crystallographic Computing Package[31] or the SHELXTL PLUS program set.[32] The analytical scattering factors for neutral atoms were used throughout the analysis;[33a] both the real ($\Delta f'$) and imaginary ($i\Delta f''$) components of anomalous dispersion[33b] were included. The quantity minimized during least-squares analysis was $\sum w(\lvert F_o\rvert - \lvert F_c\rvert)^2$, where $w^{-1} = \sigma^2(\lvert F_o\rvert) + 0.0003(\lvert F_o\rvert)$.[31]

The structure was solved by direct methods (SHELXTL PLUS) and refined by full-matrix least-squares techniques. Hydrogen atoms were included using a riding model with *d*(C–H) = 0.96 Å and *U*(iso) = 0.08 Å^2. The molecule is polymeric, with repeat units attached to each other through the cyclopentadienyl ring C(11)–C(20). Refinement of positional and thermal parameters for all non-hydrogen atoms led to convergence. The absolute structure could not be determined from the diffraction experiment either by refinement of the Rogers η parameter[34] or by inversion of the model $(-x, -y, -z)$. A final difference-Fourier synthesis yielded ρ(max) = 0.50 e Å^{-3}.

$Cp^*_2Ce[N(SiMe_3)_2]$ (6). In the glovebox, $KN(SiMe_3)_2$ (1.0 mL of a 0.50 M solution in toluene, 0.50 mmol) was added to a yellow slurry of $Cp^*_2CeCl_2K(THF)$ (275 mg, 0.414 mmol) in toluene (10 mL). The reaction mixture turned red immediately and was stirred for 30 min. The mixture was then centrifuged to remove solids (KCl), and the resulting solution was dried under vacuum to give red solids. The red solids were extracted with hexanes and centrifuged to remove excess solid $KN(SiMe_3)_2$. Solvent was removed from the red hexane solution by rotary evaporation to yield red **6** (233 mg, 0.408 mmol, 99%). ^{1}H NMR (C_6D_6): δ −11.54 (br, $\Delta\nu_{1/2}$ = 380 Hz, 18 H, $SiMe_3$), 3.58 (s, 30 H, Cp*). ^{13}C NMR (C_6D_6): δ −5.6 (q, J = 114 Hz, $SiMe_3$), 8.4 (q, J = 125 Hz, C_5Me_5), 178.8 (s, C_5Me_5). Anal. Calcd for $C_{26}H_{48}NSi_2Ce$: C, 54.69; H, 8.47; N, 2.46; Si, 9.84; Ce, 24.54. Found: C, 53.48; H, 7.87; N, 2.54; Si, 5.59; Ce, 27.50.

$Cp^*_2Nd[N(SiMe_3)_2]$ (7). $KN(SiMe_3)_2$ (1.0 mL of a 0.50 M solution in toluene, 0.50 mmol) was added to a blue slurry of $Cp^*_2NdCl_2K(THF)$ (276 mg, 0.413 mmol) in toluene (10 mL). Using the purification procedure for **6**, blue **7** (230 mg, 0.400 mmol, 97% yield) was obtained. ^{1}H NMR (C_6D_6): δ 8.63 (s, 30 H, Cp*), −19.16 (br s, $\Delta\nu_{1/2}$ = 1100 Hz, 18 H, $SiMe_3$). ^{13}C NMR (C_6D_6): δ −15.0 (q, J = 125 Hz, C_5Me_5), −4.8 (br $\Delta\nu_{1/2}$ = 1500 Hz, $SiMe_3$), 262.5 (s, C_5Me_5). Anal. Calcd for $C_{26}H_{48}NSi_2Nd$: C, 54.30; H, 8.41; N, 2.44; Si, 9.77; Nd, 25.08. Found: C, 54.02; H, 8.40; N, 2.31; Si, 9.52; Nd, 25.40.

$Cp^*_2Sm[N(SiMe_3)_2]$ (8). $KN(SiMe_3)_2$ (1.0 mL of a 0.50 M solution in toluene, 0.50 mmol) was added to an orange slurry of $Cp^*_2SmCl_2K(THF)$ (288 mg, 0.427 mmol) in toluene (10 mL). Using the purification procedure for **6**, orange **8** (235 mg, 0.404 mmol, 95% yield) was obtained. ^{1}H NMR (C_6D_6): δ 0.78 (s, 30 H, Cp*), −4.69 (br, $\Delta\nu_{1/2}$ = 60 Hz, 18 H, $SiMe_3$). ^{13}C NMR (C_6D_6): δ 12.9 (q, J = 125 Hz, $SiMe_3$), 22.0 (q, J = 125 Hz, Cp*), 120.1 (s, Cp*). Anal. Calcd for $C_{26}H_{48}NSi_2Sm$: C, 53.73; H, 8.32; N, 2.41; Si, 9.66; Sm, 25.88. Found: C, 53.52; H, 8.20; N, 2.32; Si, 9.61; Sm, 26.10.

X-ray Data Collection, Structure Determination, and Refinement for $Cp^*_2Sm[N(SiMe_3)_2]$ (8). An orange crystal (0.17 × 0.25 × 0.37 mm) was handled as described for **5** on a Syntex $P2_1$ diffractometer (R3m/V system) equipped with a modified LT-1 low-temperature system. All 12 051 data were handled as described for **5**. Diffraction symmetry indicated a rhombohedral crystal system with systematic absences for *hkl* where $-h + k + l = 3n + 1$. The two possible space groups are the noncentrosymmetric $R3$ or the centrosymmetric $R\bar{3}$. The latter was chosen and determined to be correct by successful solution and refinement of the structure. All crystallographic calculations were performed as described above for **5**. The quantity minimized during least-squares analysis was $\sum w(\lvert F_o\rvert - \lvert F_c\rvert)^2$, where $w^{-1} = \sigma^2(\lvert F_o\rvert) + 0.0002(\lvert F_o\rvert)^2$. The structure was solved and refined as described for **5**, and hydrogen atoms were included as described above for **5**. Refinement of positional and thermal parameters led to convergence. A final difference-Fourier map was devoid of significant features; ρ(max) = 0.83 e Å^{-3}.

$Cp^*_2Ce(C{\equiv}CPh)(THF)$ (9). In a glovebox, PhC≡CH (0.5 mL, 4.6 mmol) was added to a red solution of $Cp^*_2Ce[N(SiMe_3)_2]$ (300 mg, 0.53 mmol) in 5 mL of THF in a reaction vessel sealed with a high-vacuum, greaseless stopcock. The vessel was heated to 100 °C for 30 min. The solvent and excess PhC≡CH were

(31) *UCLA Crystallographic Computing Package*; University of California: Los Angeles, 1981. Strouse, C. Personal communication.
(32) Siemens Analytical X-ray Instruments, Inc., Madison, WI, 1990.
(33) (a) *International Tables for X-ray Crystallography*; Kynoch Press: Birmingham, England, 1974; Vol. IV, pp 99–101. (b) *Ibid.*, pp 149–150.
(34) Rogers, D. *Acta Crystallogr.* **1981**, *A37*, 734–741.
(35) Nowacki, W.; Matsumoto, T.; Edenharter, A. *Acta Crystallogr.* **1967**, *22*, 935–940.

removed under vacuum to leave **9** as a red solid in quantitative yield. ^{1}H NMR (C_6D_6): δ −21.2 (br, $\Delta\nu_{1/2}$ = 1500 Hz, THF), −11.4 (br, $\Delta\nu_{1/2}$ = 130 Hz, THF), 3.63 (d, J = 8 Hz, 2H, *o*-Ph), 4.14 (s, 30H, Cp*), 5.37 (t, J = 7 Hz, 2H, *m*-Ph), 5.81 (t, J = 7 Hz, 1H, *p*-Ph). ^{1}H NMR (C_4D_8O): δ 3.19 (d, J = 7 Hz, 2H, *o*-Ph), 4.08 (s, 30H, Cp*), 5.42 (t, J = 7 Hz, 2H, *m*-Ph), 5.92 (t, J = 7 Hz, 1H, *p*-Ph). ^{13}C{^{1}H} NMR (C_4D_8O): δ 12.1 (C_5Me_5), 120 (Ph), 123.0 (Ph), 123.2 (Ph), 126.5 (C_5Me_5), 127.1 (Ph), 159.4 (C≡C). IR (thin film): 3307 w, 3291 w, 3008 w, 2965 s, 2917 s, 2909 s, 2857 s, 1488 w, 1443 m, 1376 m, 1072 w, 1027 m, 946 m, 757 m, 691 m, 658 s cm^{-1}. Anal. Calcd for solvated $C_{32}H_{43}OCe$ (unsolvated $C_{28}H_{35}Ce$): C, 65.83 (65.72); H, 7.42 (6.89); Ce, 24.00 (27.38). Found: C, 63.04; H, 6.85; Ce, 26.85.

Cp*$_2$Nd(C≡CPh)(THF) (10). As described for **9**, PhC≡CH (1.0 mL, 9.1 mmol) reacted with Cp*$_2$Nd[N(SiMe$_3$)$_2$] (500 mg, 0.87 mmol) in 10 mL of THF to form blue **10** in quantitative yield. ^{1}H NMR (C_6D_6): δ −37.23 (br, 4 H, THF), −13.22 (br, 4 H, THF), 4.29 (br d, J = 7 Hz, 2 H, *o*-Ph), 5.33 (br t, J = 6 Hz, 2 H, *p*-Ph), 5.99 (br t, J = 6 Hz, 1 H, *p*-Ph), 5.99 (br t, J = 6 Hz, 1 H, *p*-Ph), 8.37 (br, 30 H, Cp*). ^{13}C NMR (C_6D_6): δ −12.9 (q, J = 122 Hz, C_5Me_5), −6.1 (br, THF), 3.0 (br, THF), 105.1 (s, C_6H_5-*i*), 113.0 (d,J = 159 Hz, C_6H_5), 121.5 (d, J = 165 Hz, C_6H_5-*p*), 126.9 (d, J = 179 Hz, C_6H_5), 128.9 (s, C_5Me_5), 148.3 (s, C≡CPh), 302.1 (s, *C*≡CPh). IR (thin film): 3074 s, 3056 s, 2923 s, 2872 s, 2855 s, 1594 m, 1484 s, 1441 s, 1377 w, 1193 m, 1058 m, 1053 s, 1026 m, 898 w, 771 m, 756 s, 693 s cm^{-1}. Anal. Calcd for solvated $C_{32}H_{43}ONd$ (unsolvated $C_{28}H_{35}Nd$): C, 65.38 (65.20); H, 7.37 (6.84); Nd, 24.53 (27.96). Found: C, 59.35; H, 6.88; Nd, 27.50. The THF-d_8 analogs of **9** and **10** were prepared by dissolving the samples in THF-d_8, stirring for 5 min, and removing the solvent by rotary evaporation.

[Cp*$_2$Ce]$_2$[μ-η^2:η^2-PhC═C═C═CPh] (11). In an NMR tube, bright red Cp*$_2$Ce(C≡CPh)(THF), (27 mg, 0.026 mmol) was dissolved in toluene-d_8 (0.5 mL). The tube was sealed with a septum and Parafilm and immersed in an oil bath at 125 °C. The reaction mixture was heated for 24 h, during which the initial bright red color slowly changed to dark red. NMR spectroscopy indicated 90% conversion to **11**. Dark green-red crystals of **11** formed in the NMR tube at room temperature. ^{1}H NMR (THF-d_8): δ −0.49 (br s, 2H, Ph), 2.72 (br s, 2H, Ph), 3.06 (br s, 30H, Cp*). ^{13}C{^{1}H} NMR (THF-d_8): δ 8.5 (C_5Me_5), 118.2, 118.9, 126.0, 128.9, 129.7, 192.4 (C_5Me_5). IR (thin film): 3062 m, 2969 s, 2906 s, 2856 s, 2725 w, 2119 w, 1956 w, 1588 w, 1556 m, 1469 m, 1438 m, 1375 m, 1250 w, 1175 w, 1156 w, 1069 s, 1025 w, 1006 w, 950 w, 787 w, 756 s, 725 w, 694 s cm^{-1}. Anal. Calcd for the ditoluene solvate $C_{70}H_{86}Ce_2$: C, 69.62; H, 7.18; Ce, 23.20. Found: C, 70.20; H, 6.44; Ce, 23.10.

[Cp*$_2$Nd]$_2$[μ-η^2:η^2-PhC═C═C═CPh] (12). As described for **11**, Cp*$_2$Nd(C≡CPh)(THF) (44 mg, 0.0427 mmol) was heated in toluene-d_8 at 125 °C for 24 h. The initial pale green color slowly turned to dark red. NMR spectroscopy indicated 85% conversion. Dark red crystals of **12** formed in the NMR tube at room temperature. ^{1}H NMR (C_6D_6): δ −60.33 (br, $\Delta\nu_{1/2}$ = 12 Hz, 2H, Ph), −7.02 (d, J = 7 Hz, 2H, Ph), −2.06 (t, J = 7 Hz, 1H, Ph), 7.88 (s, 30H, Cp*). ^{13}C{^{1}H} NMR (C_4D_8O): δ −16.1 (C_5Me_5), 117.6, 127.2, 129.4, 132.2, 267.0 (C_5Me_5). IR (thin film): 3062 w, 2968 s, 2912 s, 2863 s, 2725 w, 1587 w, 1562 m, 1444 s, 1375 m, 1256 w, 1175 w, 1150 w, 1093 s, 1087 m, 1031 m, 950 w, 794 w, 756 s, 725 w, 687 s cm^{-1}. [(C$_5$Me$_5$)$_2$Nd]$_2$[μ-η^2:η^2-PhC═C═C═CPh]·C$_7$H$_8$ crystallizes from toluene at −34 °C in space group $P2_1/m$ with a = 15.05 Å, b = 13.98 Å, c = 15.50 Å, β = 114.63°, V = 2966 Å^3, and Z = 2. From the crystallographic data, only the connectivity of the molecule was established. The data indicated that the complex is isostructural with [(C$_5$Me$_5$)$_2$Sm]$_2$[μ-η^2:η^2-PhC═C═C═CPh] (**2**).

Reactions of Cp*$_2$Sm(THF) with Alkynes. These reactions were carried out by stoichiometric addition of alkyne to a solution of Cp*$_2$Sm(THF) (200 mg, 0.41 mmol) in toluene (10 mL). The reaction mixture was heated to 100 °C for 1 h. In all cases, the resulting solutions were bright yellow. The solvent was removed *in vacuo* to leave a yellow oil. The yields were quantitative by NMR spectroscopy.

Cp*$_2$Sm(C≡CCH$_2$CH$_2$Ph)(THF) (13). ^{1}H NMR (C_6D_6): δ −3.00 (br, $\Delta\nu_{1/2}$ = 60 Hz, 4H, THF), −1.78 (br, $\Delta\nu_{1/2}$ = 40 Hz, 4H, THF), 1.59 (s, 30H, Cp*), 3.47 (t, J = 7 Hz, 2H, CH$_2$), 3.34 (t, J = 7 Hz, 2H, CH$_2$), 7.13 (t, J = 8 Hz, 2H, *m*-Ph), 7.41 (d, J = 8 Hz, 2H, *o*-Ph). ^{13}C NMR (C_6D_6): δ 15.7 (q, J = 125 Hz, C_5Me_5), 19.3 (t, J = 134 Hz, CH$_2$), 21.2 (t, J = 128 Hz, CH$_2$), 37.7 (t, J = 124 Hz, THF), 1.2 (t, J = 148 Hz, THF), 114.9 (s, C_5Me_5), 124.9 (d, J = 157 Hz, Ph), 125.6 (s), 127.3 (d, J = 157 Hz, Ph), 128.1 (s), 130.8 (d, J = 163 Hz, Ph), 141.8 (s). IR (thin film): 703 s, 751 s, 859 s, 950 w, 971 w, 1016 s, 1088 m, 1149 w, 1252 w, 1341 w, 1376 w, 1453 m, 1497 m, 2073 m, 2857 s, 2898 s, 2904 s, 2924 s, 2961 s, 3028 w cm^{-1}.

Cp*$_2$Sm(C≡CCH$_2$NEt$_2$)(THF) (14). ^{1}H NMR (C_6D_6): δ −2.92 (br, $\Delta\nu_{1/2}$ = 60 Hz, 4H, THF), −1.72 (br, $\Delta\nu_{1/2}$ = 40 Hz, 4H, THF), 1.34 (t, J = 7 Hz, 4H, NCH$_2$*C*H$_3$), 1.59 (s, 30H, Cp*), 3.03 (q, J = 7 Hz, 4H, N*C*H$_2$CH$_3$), 4.46 (s, 2H, C≡C*C*H$_2$). ^{13}C NMR (C_6D_6): δ 13.7 (q, J = 125 Hz, CH$_2$*C*H$_3$), 16.8 (q, J = 125 Hz, C_5Me_5), 20.5 (br, $\Delta\nu_{1/2}$ = 20 Hz, THF), 41.7 (t, J = 126 Hz, C≡C*C*H$_2$N), 48.0 (t, J = 132 Hz, *C*H$_2$CH$_3$), 62.5 (t, J = 130 Hz, THF), 116.0 (s, C_5Me_5). IR (thin film): 730 w, 888 m, 923 m, 978 w, 1022 s, 1058 w, 1090 w, 1197 w, 1315 m, 1351 w, 1378 m, 1437 m, 1450 m, 1455 m, 2056 w, 2724 w, 2858 s, 2871 s, 2900 s, 2905 s, 2915 s, 2967 s cm^{-1}. Anal. Calcd for $C_{31}H_{50}OSm$: C, 63.19; H, 8.55; Sm, 25.53. Found: C, 61.86; H, 8.16; Sm, 25.15.

Cp*$_2$Sm(C≡CCH$_2$CH$_2$CHMe$_2$)(THF) (15). ^{1}H NMR (C_6D_6): δ −2.98 (br, $\Delta\nu_{1/2}$ = 40 Hz, 4H, THF), −1.83 (br, $\Delta\nu_{1/2}$ = 20 Hz, 4H, THF), 1.05 (d, J = 7 Hz, 6H, Me), 1.62 (s, Cp*), 2.00 (m, 2H, CH$_2$*C*H$_2$CH), 2.11 (m, 1H, CH), 3.25 (t, J = 7 Hz, 2H, C*H*$_2$CH$_2$-CH). ^{13}C{^{1}H} NMR (C_6D_6): δ 16.8 (C_5Me_5), 18.5 (s, THF), 20.2 (CH), 22.7 (CH$_2$), 27.7 (CH$_3$), 41.3 (CH$_2$), 62.2 (s, THF), 115.8 (C_5Me_5), 131.9 (C≡C), 137.8 (C≡C). IR (thin film): 817 w, 1011 m, 1020 w, 1066 w, 1089 m, 1249 w, 1364 w, 1366 w, 1376 w, 1438 m, 1448 m, 1457 m, 1465 m, 2858 s, 2859 s, 2909 s, 2917 s, 2925 s, 2959 s cm^{-1}. Anal. Calcd for the desolvate $C_{27}H_{41}Sm$: C, 62.85; H, 8.01; Sm, 29.15. Found: C, 59.48; H, 7.20; Sm, 29.85.

Cp*$_2$Sm(C≡CCHMe$_2$)(THF) (16). ^{1}H NMR (C_6D_6): δ −3.00 (br s, 4H, THF), −1.83 (br s, 4H, THF), 1.60 (s, 30H, Cp*), 1.74 (d, J = 5 Hz, 6H, Me), 3.52 (septet, J = 7 Hz, CH). ^{13}C{^{1}H} NMR (C_6D_6): δ 16.7 (C_5Me_5), 20.2 (Me), 21.6 (CH), 26.3 (THF), 62.1 (THF), 115.8 (C_5Me_5).

[Cp*$_2$Sm(C≡CCMe$_3$)]$_2$ (17) and Cp*$_2$Sm[Me$_3$CCH═CC(CMe$_3$)═CH$_2$] (18). An excess of Me$_3$CC≡CH (1.0 mL) was added dropwise to an orange solution of [Cp*$_2$Sm(μ-H)]$_2$ (100 mg, 0.12 mmol) in 1 mL of toluene. The solution immediately turned dark yellow and evolved gas. The reaction mixture was stirred for 5 min, and solvent was removed under vacuum. The yellow-orange oil was then extracted with hexanes. This solid material was recrystallized from toluene at −35 °C. Yellow crystals of [Cp*$_2$Sm(C≡CCMe$_3$)]$_2$ and orange crystals of Cp*$_2$Sm[Me$_3$CCH═CC(CMe$_3$)═CH$_2$] were then obtained. Attempts to generate pure samples of **17** from Cp*$_2$Sm or [Cp*$_2$Sm(μ-H)]$_2$ with Me$_3$CC≡CH at low temperatures or pure samples of **18** from Cp*$_2$Sm, Me$_3$CC≡CH, and Me$_3$CCH═CH$_2$ also generated mixtures of products.

X-ray Data Collection, Structure Determination, and Refinement for [Cp*$_2$Sm(C≡CCMe$_3$)]$_2$ (17). A yellow crystal (0.23 × 0.28 × 0.30 mm) was handled as described for **5**, and details appear in Table I. All 9287 data were corrected for absorption and for Lorentz and polarization effects and placed on an approximately absolute scale. Any reflection with I(net) < 0 was assigned the value $|F_o| = 0$. There were no systematic extinctions nor any diffraction symmetry other than the Friedel condition. The two possible triclinic space groups are the noncentrosymmetric $P1$ [C^1_1; No. 1] or the centrosymmetric $P\bar{1}$ [C^1_i; No. 2]. With Z = 4 and no expectation of a resolved chiral molecule, the latter centrosymmetric space group is far more probable[35] and was later shown to be the correct choice.

All crystallographic calculations were performed as described above for **5**. The quantity minimized during least-squares analysis was $\sum w(|F_o| - |F_c|)^2$, where $w^{-1} = \sigma^2(|F_o|) + 0.0002(|F_o|)^2$. The structure was solved and refined as described for **5**, and hydrogen atoms were included as described above for **5**. There are two

independent molecules in the asymmetric unit. A final difference-Fourier map yielded ρ(max) = 0.64 e Å^{-3}.

X-ray Data Collection, Structure Determination, and Refinement for $Cp^*_2Sm[RCH{=}CC(R){=}CH_2]$ (R = CMe_3; 18). An orange crystal (0.20 × 0.30 × 0.33 mm) was handled as described for 8, and details appear in Table I. All 4405 data were corrected for absorption and for Lorentz and polarization effects and placed on an approximately absolute scale. A careful examination of a preliminary data set revealed the systematic extinctions $0kl$ for $k = 2n + 1$, $h0l$ for $l = 2n + 1$, and $hk0$ for $h = 2n + 1$. The centrosymmetric orthorhombic space group $Pbca$ [D^{15}_{2h}; No. 61] is thus uniquely defined.

All crystallographic calculations were performed as described above for 5. The quantity minimized during least-squares analysis was $\sum w(|F_o| - |F_c|)^2$, where $w^{-1} = \sigma^2(|F_o|) + 0.0005(|F_o|)^2$. The structure was solved and refined as described for 5, and hydrogen atoms were included as described above for 5. A final difference-Fourier map was devoid of significant features; ρ(max) = 1.12 e Å^{-3}.

$[Cp^*_2Sm]_2[\mu$-η^2:η^2-$Ph(CH_2)_2C{=}C{=}C{=}C(CH_2)_2Ph]$ (19). In a glovebox, an NMR tube was charged with Cp^*_2Sm (9 mg, 0.021 mmol) and C_7D_8 (0.5 mL) and capped with a septum. A syringe containing $PhCH_2CH_2C{\equiv}CH$ (3.5 μL, 0.025 mmol) was inserted through the septum, and the tube was cooled to −78 °C. The alkyne was added, and the solution was shaken vigorously. Gas evolution was observed, and the reaction mixture turned from dark green to pale yellow-green. After 10 min, the mixture was warmed slowly to room temperature over a period of 20 min. When it was warmed, the solution slowly turned red and then dark red. NMR spectroscopy indicated quantitative formation of 19. Crystals suitable for X-ray analysis were grown from toluene at −34 °C. ^{1}H NMR (C_6D_6): δ −12.94 (br, $\Delta\nu_{1/2}$ = 20 Hz, 2H, CH_2), −1.48 (br, $\Delta\nu_{1/2}$ = 20 Hz, 2H, CH_2), 1.47 (s, 30H, Cp*), 4.91 (d, J = 8 Hz, 2H, Ph), 6.29 (t, J = 7 Hz, 2H, Ph), 6.38 (t, J = 7 Hz, 1H, Ph). ^{1}H NMR (C_4D_8O): δ −10.71 (br, $\Delta\nu_{1/2}$ = 140 Hz, 2H, CH_2), −1.10 (br, $\Delta\nu_{1/2}$ = 70 Hz, 2H, CH_2), 1.44 (s, 30H, Cp*), 5.50 (d, J = 7 Hz, 2H, Ph), 6.59 (t, J = 7 Hz, 2H, Ph), 6.65 (t, J = 7 Hz, 1H, Ph)). ^{13}C{^{1}H} NMR (C_4D_8O): δ 17.5 (C_5Me_5), 114.5 (C_5Me_5), 125.4 (Ph), 126.6 (Ph), 128.0 (Ph), 129.1 (CH_2), 139.2 (CH_2). Anal. Calcd for $C_{30}H_{39}Sm$: C, 65.51; H, 7.15; Sm, 27.35. Found: C, 63.35; H, 6.92; Sm, 27.50.

X-ray Data Collection, Structure Determination, and Refinement for $[Cp^*_2Sm]_2[\mu$-η^2:η^2-$PhCH_2CH_2C{=}C{=}C{=}CCH_2CH_2Ph]$ (19). A red crystal (0.20 × 0.23 × 0.37 mm) was handled as described for 8, and details appear in Table I. All 6046 data were corrected for absorption and for Lorentz and polarization effects and placed on an approximately absolute scale. Any reflection with I(net) < 0 was assigned the value $|F_o| = 0$. The systematic extinctions observed were hkl for $h + k = 2n + 1$ and $h0l$ for $l = 2n + 1$; the diffraction symmetry was $2/m$. The two possible monoclinic space groups are Cc [C^4_s; No. 9] and $C2/c$ [C^6_{2h}; No. 15]. The centrosymmetric space group $C2/c$ was later determined to be the correct choice. All crystallographic calculations were carried out as described for 5.

The structure was solved and refined as described for 5, and hydrogen atoms were included as described above for 5. The molecule is a dimer located on a 2-fold rotation axis (0, y, $^1/_4$). There are two molecules of toluene per dimeric unit. A final difference-Fourier map was devoid of significant features; ρ(max) = 1.01 e Å^{-3}.

$[Cp^*_2Sm]_2[\mu$-η^2:η^2-$Me_2CH(CH_2)_2C{=}C{=}C{=}C(CH_2)_2CHMe_2]$ (20). As described for 19, Cp^*_2Sm (64 mg, 0.15 mmol) in C_7D_8 (0.5 mL) was treated with $Me_2CHCH_2CH_2C{\equiv}CH$ (25 μL, 0.19 mmol) at −78 °C. The initially dark green solution turned pale yellow-green. The reaction mixture was kept cool for 10 min and then warmed to room temperature over a period of 20 min. At ambient temperature, the solution was dark red. NMR spectroscopy indicated quantitative formation of 20. Crystals suitable for X-ray analysis were grown from toluene at −34 °C. ^{1}H NMR (C_6D_6): δ −12.35 (br, $\Delta\nu_{1/2}$ = 20 Hz, 2H, CH_2), −2.17 (br, $\Delta\nu_{1/2}$ = 20 Hz, 2H, CH_2), 1.60 (br, $\Delta\nu_{1/2}$ = 20 Hz, 1H, CH), −1.21 (d, J = 7 Hz, 6H, Me). ^{1}H NMR (C_4D_8O): δ −10.70 (br s, 2H, CH_2), −1.69 (br s, 2H, CH_2), −0.74 (br s, 1H, CH), −0.67 (d, J = 0.4 Hz, 6H, Me), 1.45 (s, 30H, Cp*). ^{13}C{^{1}H} NMR (C_4D_8O): δ 1.67 (br, $\Delta\nu_{1/2}$ = 60 Hz, CH_2), 11.67 (CH_2), 18.43 (CH), 17.73 (C_5Me_5), 20.45 (Me), 114.57 (C_5Me_5). Anal. Calcd for $C_{54}H_{82}Sm_2$: C, 62.85; H, 8.01; Sm, 29.07. Found: C, 62.66; H, 7.85; Sm, 29.40. The material crystallized in space group $P\bar{1}$ with unit cell constants of a = 10.6650(35) Å, b = 10.9370(48) Å, c = 12.3814(58) Å, α = 68.978(32)°, β = 65.670(31)°, γ = 86.009(31)°, V = 3712 Å^3, and Z = 1.

Formation of $PhC{\equiv}CCH{=}CHPh$ from $[Cp^*_2Sm]_2[\mu$-η^2:η^2-$PhC{=}C{=}C{=}CPh]$ and $PhC{\equiv}CH$. In a glovebox, $PhC{\equiv}CH$ was added dropwise to a stirred solution of $[Cp^*_2Sm]_2[\mu$-η^2:η^2-$PhC_4Ph]$ (132 mg, 0.126 mmol) in 10 mL of THF until the solution turned from dark red to bright yellow. The solvent and excess alkyne were then removed under vacuum to leave a yellow solid whose ^{1}H NMR spectrum indicated the presence of $Cp^*_2Sm(C{\equiv}CPh)(THF)$ in the product mixture. Sublimation of the product mixture at 80 °C and 10^{-5} Torr left a yellow residue and formed a volatile component identified by mass, NMR, and IR spectroscopy as $PhC{\equiv}CCH{=}CHPh$ (21 mg, 82%). The 1:10 product ratio observed in the GC/MS may be due to *cis* and *trans* isomers, respectively, although resonances in the NMR spectrum for a *cis*-$CH{=}CH$ group were not identified. ^{1}H NMR (C_6D_6): δ 6.31 (d, J = 16.0 Hz), 7.00 (m), 7.08 (d, J = 7.0 Hz), 7.52 (d, J = 7.8 Hz), 7.53 (d, J = 7.8 Hz). IR (thin film): 3025 s, 2914 s, 2909 s, 2260 w, 1593 w, 1484 m, 1442 s, 1375 m, 1251 w, 1150 m, 1088 s, 1025 m, 1018 m, 1011 m, 950 w, 757 m, 692 m, 652 m cm^{-1}, M$^+$ ion: m/e 204.

Results and Discussion

The Samarium Phenylalkynide Coupling Reaction. Formation of $[Cp^*_2Sm]_2(\mu$-η^2:η^2-$PhC{=}C{=}C{=}CPh)$ (1) from "$Cp^*_2Sm(C{\equiv}CPh)$" and $Cp^*_2Sm(C{\equiv}CPh)(THF)$ (2). The initial report[6] of the formation of "$[Cp^*_2Sm(\mu$-$C{\equiv}CPh)]_2$" by reaction of $Cp^*_2Sm[CH(SiMe_3)_2]$ with $HC{\equiv}CPh$ (eq 13) seemed unlikely due to steric factors.

$$2Cp^*_2Sm[CH(SiMe_3)_2] + 2HC{\equiv}CPh \rightarrow \text{"}[Cp^*_2Sm(\mu\text{-}C{\equiv}CPh)]_2\text{"} \quad (13)$$

Previous structural studies of bimetallic complexes containing two Cp^*_2Sm units with small bridging ligands had shown that the four C_5Me_5 rings prefer to adopt a tetrahedral geometry.[22-24,36-40] Figure 1 shows three examples of tetrahedral tetrakis(cyclopentadienyl) complexes: $[Cp^*_2Sm]_2(\mu$-O),[36] $[Cp^*_2Sm]_2(\mu$-η^2:η^2-$N_2)$,[24] and $[Cp^*_2Sm(\mu$-H)$]_2$.[22] The four large Cp* ligands are apparently so close together that the best close-packing arrangement, tetrahedral, is preferred over the alternative square-planar orientation common for $[(C_5R_5)_2M(\mu$-Z$)]_2$ complexes (Z = monoanionic ligand).[41] The tetrahedral

(36) Evans, W. J.; Grate, J. W.; Bloom, I.; Hunter, W. E.; Atwood, J. L. *J. Am. Chem. Soc.* **1985**, *107*, 405-409.
(37) Evans, W. J.; Drummond, D. K.; Grate, J. W.; Zhang, H.; Atwood, J. L. *J. Am. Chem. Soc.* **1987**, *109*, 3928-3936.
(38) Evans, W. J.; Ulibarri, T. A.; Ziller, J. W. *J. Am. Chem. Soc.* **1990**, *112*, 2314-2324.
(39) See also: Evans, W. J.; Peterson, T. T.; Rausch, M. D.; Hunter, W. E.; Zhang, H.; Atwood, J. L. *Organometallics* **1985**, *4*, 554-559.
(40) In contrast, see: Evans, W. J.; Gonzales, S. L.; Ziller, J. W. *J. Am. Chem. Soc.* **1991**, *113*, 9880-9882.
(41) For example: (a) Jungst, R.; Sekutowski, D.; Davis, J.; Luly, M.; Stucky, G. D. *Inorg. Chem.* **1977**, *16*, 1645-1655. (b) Wielstra, Y.; Gambarotta, S.; Meetsma, A.; de Boer, J. L. *Organometallics* **1990**, *8*, 250-251. (c) Chiang, M. Y.; Gambarotta, S.; Van Bolhuis, F. *Organometallics* **1988**, *7*, 1864-1865. (d) Payne, R.; Hachgenei, J.; Fritz, G.; Fenske, D. Z. *Naturforsch.* **1986**, *41B*, 1535-1540. (e) Bottomley, F.; Drummond, D. F.; Egharevba, G. O.; White, P. S. *Organometallics* **1986**, *5*, 1620-1625. (f) Hey, E.; Lappert, M. F.; Atwood, J. L.; Bott, S. G. *J. Chem. Soc., Chem. Commun.* **1987**, 421-422. (g) Hencken, G.; Weiss, E. *Chem. Ber.* **1973**, *106*, 1747-1751. See also: Lauher, J. W.; Hoffmann, R. *J. Am. Chem. Soc.* **1976**, *98*, 1729-1742.

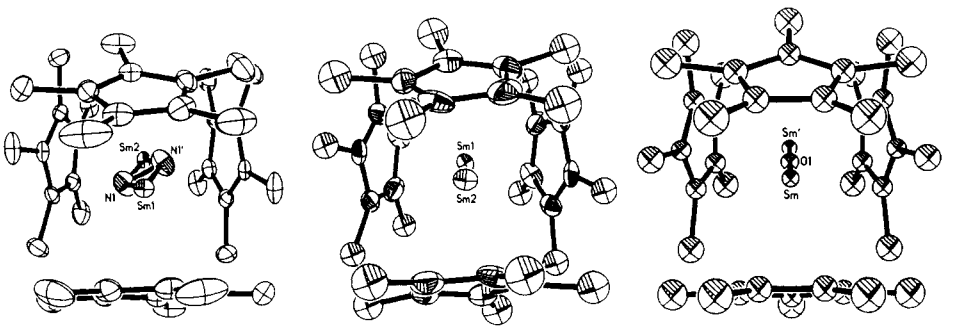

Figure 1. Views down the Sm–Sm vectors of $[(C_5Me_5)_2Sm]_2(\mu\text{-}\eta^2\text{:}\eta^2\text{-}N_2)$, $[(C_5Me_5)_2Sm(\mu\text{-}H)]_2$, and $[(C_5Me_5)_2Sm]_2(\mu\text{-}O)$.

tetrakis(cyclopentadienyl) ligand environment formed by two Cp^*_2Sm units did not seem to be large enough to accommodate two symmetrically bridging C≡CPh ligands in a molecule such as "$[Cp^*_2Sm(\mu\text{-}C{\equiv}CPh)]_2$". Hence, in contrast to the bridged alkynide complexes of samarium containing smaller cyclopentadienyl ligand, i.e., the crystallographically characterized $[(MeC_5H_4)_2Sm(\mu\text{-}C{\equiv}C\text{-}CMe_3)]_2$[42] and $[(Me_3CC_5H_4)_2Sm(\mu\text{-}C{\equiv}CPh)]_2$,[43] an alternative structure was expected for "$[Cp^*_2Sm(\mu\text{-}C{\equiv}CPh)]_2$". This expectation was further supported by the fact that this complex was reported to be red, whereas Sm(III) alkynides are more typically yellow[26,42,43] and the complex did not exhibit any $\nu_{C\equiv C}$ stretch in its infrared spectrum.

Reinvestigation[14] of the $Cp^*_2Sm[CH(SiMe_3)_2]$/HC≡CPh reaction showed that the product was the diphenylbutatrienediyl derivative, $[Cp^*_2Sm]_2(PhC{=}C{=}C{=}CPh)$ (**1**; eq 2), a red complex that had been previously obtained[16] from diphenylbutadiyne and $Cp^*_2Sm(THF)_2$ (eq 14). Hence, the "$Cp^*_2Sm(C{\equiv}CPh)$" moiety expected from eq 2 generated a coupled dianionic $(PhC{=}C{=}C{=}CPh)^{2-}$ ligand instead of forming a bridged dimer which would be sterically unfavorable.

$$2Cp^*_2Sm(THF)_2 + PhC{\equiv}CC{\equiv}CPh \rightarrow [Cp^*_2Sm]_2(\mu\text{-}\eta^2\text{:}\eta^2\text{-}PhC{=}C{=}C{=}CPh) \quad (14)$$
$$\mathbf{1}$$

To fully establish that a $(PhC{\equiv}C)^-$ to $(PhC{=}C{=}C{=}CPh)^{2-}$ transformation had occurred, the reactivity of the crystallographically characterized samarium phenylalkynide complex $Cp^*_2Sm(C{\equiv}CPh)(THF)$ (**2**)[26] was examined. At 120 °C in a sealed NMR tube in benzene, **2** is converted in 40% yield over 3 days to **1** (eq 5). At 145 °C in toluene, **1** is formed quantitatively in 14 h. No evidence for the **1** → **2** back-reaction has been observed, although **1** does appear to transform to other products at these temperatures in THF.

The conversion of **2** to **1** does not occur in THF, and therefore, THF dissociation appears to be a critical step in the reaction. The initial rates of formation of **1** are directly proportional to the initial concentration of $Cp^*_2Sm(C{\equiv}CPh)(THF)$, but after about 50% conversion the rate drops dramatically, presumably due to the buildup of THF. At 100 °C, an initial rate of formation of 5.7×10^{-6} M s^{-1} is observed up to 50% conversion, but the rate then diminishes, such that conversion beyond 80% is not achieved. No reaction is observed when the reaction is attempted at 100 °C in the presence of 0.5 equiv of THF. These data are consistent with dissociation of THF as the first step in the reaction.

Scheme I

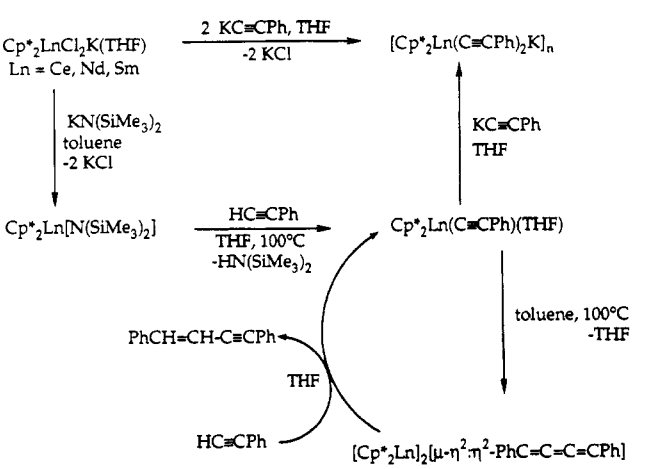

These data, along with the fact that the formation of **1** was neither detected nor predicted in a detailed thermodynamic study[6] of "$[Cp^*_2Sm(\mu\text{-}C{\equiv}CPh)]_2$", suggested that once "$Cp^*_2Sm(C{\equiv}CPh)$" is formed, it is converted very easily to **1**. Hence, the rate-determining step appeared to be the formation of "$Cp^*_2Sm(C{\equiv}CPh)$" and the subsequent coupling reaction would not provide readily accessible kinetic information. Accordingly, we turned our attention to the effect of the metal and the alkynide substituent on this reaction.

Cerium and Neodymium Phenylalkynides. A summary of the reactions discussed below is given in Scheme I.

(a) Synthetic Considerations. To determine if the coupling reaction in eqs 2–5 involved the divalent oxidation state of samarium, it was desirable to examine the chemistry of analogs of $Cp^*_2Sm(C{\equiv}CPh)(THF)$ with metals which did not have a readily accessible divalent state. Since steric effects may influence this reaction, metals similar in size were desired. The two lanthanides closest in size to samarium were unsuitable due to the radioactivity of promethium and the available divalent state of europium. The next best candidate, neodymium, was chosen for examination over gadolinium since its magnetic moment was lower and characterization by NMR spectroscopy would be less difficult. Cerium complexes were also examined, since a considerable amount of structural information has been assembled on Cp* complexes of this metal.[13,44–47] The synthesis of some pen-

(42) Evans, W. J.; Bloom, I.; Hunter, W. E.; Atwood, J. L. *Organometallics* **1983**, *2*, 709–714.
(43) Shen, Q.; Zheng, D.; Lin, L.; Lin, Y. *J. Organomet. Chem.* **1990**, *391*, 307–312.

tamethylcyclopentadienyl alkynide complexes of this metal have subsequently been reported.[48]

Whereas $Cp^*_2Sm(C{\equiv}CPh)(THF)$ is easily synthesized from $Cp^*_2Sm(THF)_2$ and $HC{\equiv}CPh$ (eq 15), this convenient divalent route to the cerium and neodymium analogs is not available. Normally, the most straightforward route

$$Cp^*_2Sm(THF)_2 + HC{\equiv}CPh \rightarrow Cp^*_2Sm(C{\equiv}CPh)(THF) \quad (15)$$

to these complexes would be an ionic metathesis reaction involving $MC{\equiv}CPh$ (M = alkali metal) and a bis(cyclopentadienyl)lanthanide halide.[49] However, the reaction of 2 equiv of MCp* with $LnCl_3$ to form the requisite $Cp^*_2LnCl(THF)$ precursor typically generates the alkali-metal adduct $Cp^*_2LnCl_2M(THF)_2$.[29,39,45–47,50] Conversion of $Cp^*_2LnCl_2M(THF)_2$ to $Cp^*_2LnCl(THF)$ often occurs in low yield.[51] In addition, reaction of $Cp^*_2LnCl(THF)$ with $MC{\equiv}CPh$ could generate the alkali-metal halide adduct $Cp^*_2LnCl(C{\equiv}CPh)M(THF)_2$[52] (see below). The reaction of $HC{\equiv}CPh$ with a suitable $Cp^*_2LnZ(THF)$ complex would be a better route, but for Z = H or alkyl, the Cp^*_2LnZ complexes are such active metalation reagents that they can react with THF.[27,53–55] Hence, to obtain a clean, high-yield synthesis, the reaction of Cp^*_2LnZ complexes with $HC{\equiv}CPh$ would optimally be done in the absence of THF,[56] and the "$Cp^*_2Ln(C{\equiv}CPh)$" intermediate formed could convert to a trienediyl complex before isolation of the alkynide was achieved. In addition these complexes could yield a mixture of products due to competitive insertion reactions (see below).[48,57]

To avoid these problems, we sought to develop other synthetic routes to $Cp^*_2Ln(C{\equiv}CPh)(THF)$ complexes which conveniently used the readily obtained $Cp^*_2LnCl_2M(THF)_2$ complexes as precursors. Two approaches to this goal are described below. The first method provided only the bis(alkynide) complexes $[Cp^*_2Ln(C{\equiv}CPh)_2]^-$. However, these complexes were independently interesting since they provided the opportunity to determine if the two adjacent $(C{\equiv}CPh)^-$ ligands would couple to form $(PhC{=}C{=}C{=}CPh)^{2-}$ in this monometallic environment. The second method, which was based on amide chemistry, provided the best route to the $Cp^*_2Ln(C{\equiv}CPh)(THF)$ complexes. Since the NMR resonances of cerium and neodymium complexes are broader and more shifted than those of samarium complexes, the samarium analogs were studied first to establish the synthetic details which were then used for the other metals.

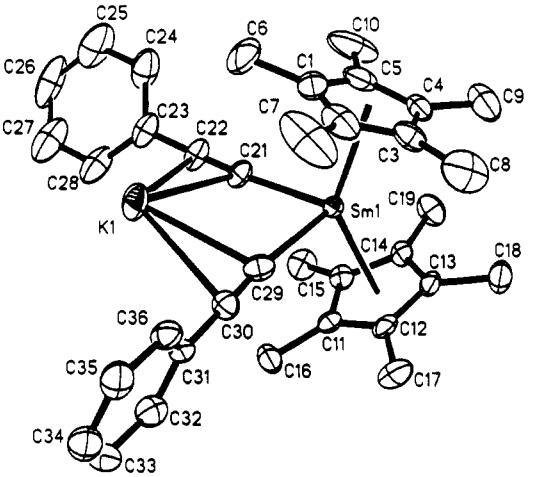

Figure 2. Molecular structure of $[(C_5Me_5)_2Sm(C{\equiv}CPh)_2K]_n$ (5), with probability ellipsoids drawn at the 50% level.

(b) $[Cp^*_2Ln(C{\equiv}CPh)_2K]_n$ Complexes. (i) Synthesis. The complexes $Cp^*_2LnCl_2K(THF)_2$ (Ln = Sm, Nd, Ce) were synthesized from $LnCl_3$ and KC_5Me_5 by following the literature method used for the lithium analogs.[29] These KCl adducts react cleanly with 2 equiv of $KC{\equiv}CPh$ in toluene to form $[Cp^*_2Ln(C{\equiv}CPh)_2K]_n$ (eq 16). Reactions

$$Cp^*_2LnCl_2K(THF)_2 + 2KC{\equiv}CPh \rightarrow (1/n)[Cp^*_2Ln(C{\equiv}CPh)_2K]_n + 2KCl \quad (16)$$

3–5

Ln = Ce (**3**), Nd (**4**), Sm (**5**)

of 1 equiv of $KC{\equiv}CPh$ with $Cp^*_2LnCl_2K(THF)_2$ did not form $Cp^*_2Ln(C{\equiv}CPh)(THF)$ but instead gave mixtures containing the bis(alkynide) $[Cp^*_2Ln(C{\equiv}CPh)_2K]_n$ and unreacted starting material. Reactions of $Cp^*_2LnCl(THF)$ with $KC{\equiv}CPh$ also gave $[Cp^*_2Ln(C{\equiv}CPh)_2K]_n$. As anticipated above, there is a strong tendency for the alkali-metal reagent to form alkali-metal adducts.

The intensely colored blue cerium (**3**), green neodymium (**4**), and orange samarium (**5**) $[Cp^*_2Ln(C{\equiv}CPh)_2K]_n$ complexes obtained via eq 16 were surprisingly soluble in arene solvents, considering that their $Cp^*_2LnCl_2K(THF)_2$ chloride analogs had little arene solubility. Although analytical data were consistent with the presence of THF in the intially isolated product, the ^1H NMR spectra in C_6D_6 of samples recrystallized from toluene indicated that no THF was present. To determine why these complexes lacked the THF expected to complete the coordination sphere of the potassium ions, X-ray crystallographic studies were carried out. The samarium derivative provided the best structural data.

(ii) Structure of $[Cp^*_2Sm(C{\equiv}CPh)_2K]_n$ (5). The molecular structure of $[Cp^*_2Sm(C{\equiv}CPh)_2K]_n$ is shown in Figure 2, and a diagram of the polymeric nature of this complex is presented in Figure 3. The coordination

(44) Renkema, J.; Teuben, J. H. *Recl. Trav. Chim. Pays-Bas* **1986**, *105*, 241–242. Heeres, H. J.; Meetsma, J.; Teuben, J. H. *J. Chem. Soc., Chem. Commun.* **1988**, 962. Heeres, H. J.; Meetsma, A.; Teuben, J. H.; Rogers, R. D. *J. Organomet. Chem.* **1989**, *364*, 87–96. Heeres, H. J.; Renkema, J.; Booij, M.; Meetsma, A.; Teuben, J. H. *Organometallics* **1988**, *7*, 2495–2502.

(45) Hazin, P. N.; Huffman, J. C.; Bruno, J. W. *Organometallics* **1987**, *6*, 23–27. Hazin, P. N.; Lakshminarayan, C.; Brinen, L. S.; Knee, J. L.; Bruno, J. W.; Streib, W. E.; Folting, K. *Inorg. Chem.* **1988**, *27*, 1393–1400.

(46) Rausch, M. D.; Moriarty, K. J.; Atwood, J. L.; Weeks, J. A.; Hunter, W. E.; Brittain, H. G. *Organometallics* **1986**, *5*, 1281–1283.

(47) Evans, W. J.; Olofson, J. M.; Zhang, H.; Atwood, J. L. *Organometallics* **1988**, *7*, 629–633.

(48) Heeres, H. J.; Teuben, J. H. *Organometallics* **1991**, *10*, 1980–1986.

(49) Evans, W. J. In *The Chemistry of the Metal-Carbon Bond*; Hartley, F. R., Patai, S., Eds.; Wiley: New York, 1982; Chapter 12.

(50) Evans, W. J.; Boyle, T. J.; Ziller, J. W. *Inorg. Chem.* **1992**, *31*, 1120–1122 and references therein.

(51) E.g.: Evans, W. J.; Grate, J. W.; Levan, K. R.; Bloom, I.; Peterson, T. T.; Doedens, R. J.; Zhang, H.; Atwood, J. L. *Inorg. Chem.* **1986**, *25*, 3614–3619. den Haan, K. H.; Wielstra, Y.; Eshuis, J. J. W.; Teuben, J. H. *J. Organomet. Chem.* **1987**, *323*, 181–192. den Haan, K. H.; Teuben, J. H. *J. Organomet. Chem.* **1987**, *322*, 321–329.

(52) Evans, W. J.; Drummond, D. K.; Hanusa, T. P.; Olofson, J. M. *J. Organomet. Chem.* **1989**, *376*, 311–320.

(53) Evans, W. J.; Ulibarri, T. A.; Ziller, J. W. *Organometallics* **1991**, *10*, 134–142.

(54) Watson, P. L. *J. Chem. Soc., Chem. Commun.* **1983**, 276–277.

(55) den Haan, K. H.; Teuben, J. H. *Recl. Trav. Chim. Pays-Bas* **1984**, *103*, 333–334.

(56) It has subsequently been shown for cerium that $Cp^*_2Ce[CH(SiMe_3)_2]$ will react in a 10:1 pentane–THF mixture to produce $Cp^*_2Ce(C{\equiv}CPh)(THF)$ in 44% yield.[48]

(57) Heeres, H. J.; Heeres, A.; Teuben, J. H. *Organometallics* **1990**, *9*, 1508–1510.

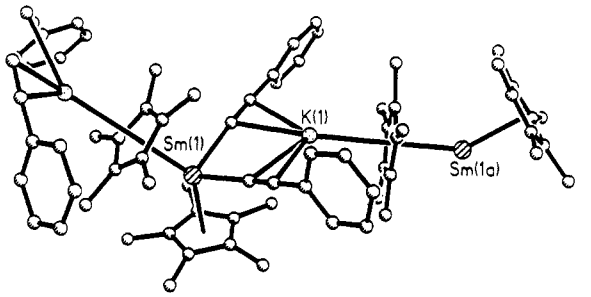

Figure 3. Ball and stick drawing showing the polymeric structure of $[(C_5Me_5)_2Sm(C{\equiv}CPh)_2K]_n$ (**5**).

Table II. Selected Interatomic Distances (Å) and Angles (deg) for $[Cp^*_2Sm(C{\equiv}CPh)_2K]_n$ (5)

Sm(1)–K(1)	4.076(2)	K(1)–C(21)	2.943(6)
Sm(1)–C(1)	2.722(7)	K(1)–C(22)	3.034(6)
Sm(1)–C(2)	2.738(7)	K(1)–C(29)	2.966(6)
Sm(1)–C(3)	2.730(6)	K(1)–C(30)	3.197(6)
Sm(1)–C(4)	2.726(6)	K(1)–C(11A)	3.202(5)
Sm(1)–C(5)	2.705(6)	K(1)–C(12A)	3.229(6)
Sm(1)–C(11)	2.752(6)	K(1)–C(13A)	3.059(5)
Sm(1)–C(12)	2.744(5)	K(1)–C(14A)	2.922(5)
Sm(1)–C(13)	2.756(5)	K(1)–C(15A)	3.010(6)
Sm(1)–C(14)	2.754(5)	C(21)–C(22)	1.213(9)
Sm(1)–C(15)	2.755(6)	C(22)–C(23)	1.447(9)
Sm(1)–C(21)	2.491(6)	C(29)–C(30)	1.200(8)
Sm(1)–C(29)	2.490(6)	C(30)–C(31)	1.446(8)
C(21)–Sm(1)–C(29)	90.0(2)	C(21)–C(22)–C(23)	177.4(6)
C(21)–K(1)–C(22)	23.3(2)	C(22)–C(23)–C(24)	119.4(7)
C(21)–K(1)–C(29)	73.2(2)	K(1)–C(29)–C(30)	89.9(4)
C(22)–K(1)–C(29)	96.3(2)	K(1)–C(30)–C(29)	68.1(4)
C(21)–K(1)–C(30)	94.2(2)	K(1)–C(30)–C(31)	110.7(4)
C(22)–K(1)–C(30)	116.6(2)	C(29)–C(30)–C(31)	178.1(6)
C(29)–K(1)–C(30)	22.1(2)		

geometry around samarium is similar to that in $Cp^*_2Y(C{\equiv}CCMe_3)_2Li(THF)$ (**21**),[52] except that the alkali metal in **5** is η^5-coordinated to a Cp* ring instead of a solvent molecule. This η^5-coordination creates a polymeric structure and explains why no THF was observed in NMR samples of this complex crystallized from arenes. Crystallographic data on $[Cp^*_2Ce(C{\equiv}CPh)_2K]_n$ (**3**) revealed the same structural features, but disorder in the Cp* rings limited the quality of the structure.

Complex **5** differs from **21** in that the C_5Me_5 rings are staggered, not eclipsed. This may occur due to the larger size of the alkali metal in **5**, which gives different angles in the $M_2(\mu$-alkynide carbon$)_2$ rhombus: 90.0(2)° for C(21)–Sm–C(29) (vs an 84.8(10)° analogous angle in **21**) and 73.2(2)° for C(21)–K–C(29) (vs 100.0(22)° in **21**). The Cp*(ring centroid)–Ln–Cp*(ring centroid) angles are 140.7° in **5** and 138.3° in **21**.

The Ln–C(Cp*) bond distances (Table II) in **5** and **21**, 2.724(11) and 2.65(1) Å, respectively, are similar, considering that yttrium is 0.06 Å smaller in radial size.[58] The 2.752(5) Å Sm–C(bridging ring) average distance is larger, as is typical for a bridging ligand.[59-61] This difference is not as great as expected, however. For example, the difference in terminal and bridging Yb–C(ring) distances in $[(C_5H_4Me)(THF)Yb(\mu\text{-}C_5H_4Me)]_n$ is 0.11–0.15 Å.[59]

The Ln–C(alkynide) distances of **5** (2.490(6) Å) and **21** (2.38(2) Å) show a discrepancy greater than the difference in ionic radii. Hence, the phenylalkynide bond distance in **5** is longer than the analogous *tert*-butylalkynide length in **21**. A long samarium *phenyl*alkynide bond was also found in $Cp^*_2Sm(C{\equiv}CPh)(THF)$ (**2**). Interestingly, the bridging Sm–C(alkynide) distance in **5** is the *same* as the terminal Sm–C(alkynide) distance in **2** (2.49(2) Å). This is a rare example contradicting the usual trend that bonds to bridging ligands tend to be longer than bonds to the same ligand in a terminal position.[60,61]

The potassium atom in **5** is not as symmetrically located as the lithium in **21**, which has Y, Li, and the α- and β-carbon atoms of both alkynides in a crystallographic mirror plane. The potassium in **5** lies 0.79 Å below the plane defined by samarium and the two α-alkynide carbons. One β-carbon (C(30)) lies 0.13 Å above this plane, and the other β-carbon (C(22)) lies 0.11 Å below the plane. Although the two α-carbon distances are equivalent (2.941(6) and 2.966(6) Å), the β-carbon distances (3.034(6) and 3.197(6) Å) are such that the metal is closer to the C(21)–C(22) bond. Neither the C≡C bond lengths (1.213(9) and 1.200(8) Å) nor the Sm–C–C angles (174.9(5) and 172.4(5)°) reflect this difference. The C≡C distances in **5** are comparable to that in **21** (1.24(2) Å) and differ from those in the two molecules in the unit cell of $Cp^*_2Sm(C{\equiv}CPh)(THF)$ (1.11(2) and 1.13(2) Å). The K–C(ring) distances average 3.08(13) Å, which can be compared to the 3.030-Å average distance in polymeric $[(\mu\text{-}\eta^5{:}\eta^5\text{-}C_5Me_5)K(pyridine)_2]_n$ (**22**).[62] The individual K–C(ring) distances vary over a wider range (2.922(5)–3.229(6) Å) than in **22** (2.962(2)–3.104(2) Å). The shorter K–C(Cp*) distances in **5** involve C(14a) and C(15a), the carbons nearest the β alkynide carbon furthest away from potassium. This asymmetry is consistent with the fact that the potassium–Cp*(ring centroid)–samarium angle (171.6°) is not perfectly linear. The observed asymmetry may simply maximize the saturation of the coordination sphere of potassium.

(iii) Reactivity of $[Cp^*_2Sm(C{\equiv}CPh)_2K]_n$. Complex **5** failed to convert to either $Cp^*_2Sm(C{\equiv}CPh)(THF)$ (**2**) or $[Cp^*_2Sm]_2(\mu\text{-}\eta^2{:}\eta^2\text{-}PhC{=}C{=}C{=}CPh)$ (**1**) under thermolytic conditions. Heating **5** to 190 °C under vacuum (5×10^{-6} Torr) or to 130 °C in toluene for 3 days gave only decomposition products; **1** was not detected. When **5** is heated in THF at reflux, it is recovered unchanged. Hence, having two alkynide units to close proximity in the coordination environment of samarium is not sufficient to cause coupling.

In the case of samarium, the potassium-free alkynide complex $Cp^*_2Ln(C{\equiv}CPh)(THF)$ can be obtained from $[Cp^*_2Ln(\mu\text{-}C{\equiv}CPh)_2K]_n$ as a precursor using the previously characterized cation $[Cp^*_2Sm(THF)_2][BPh_4]$,[26] as shown in eq 17. This synthetic route was not extended to

$$(1/n)[Cp^*_2Sm(\mu\text{-}C{\equiv}CPh)_2K]_n + [Cp^*_2Sm(THF)_2][BPh_4] \rightarrow 2Cp^*_2Sm(C{\equiv}CPh)(THF) + KBPh_4 \quad (17)$$

cerium and neodymium, however, since the analogous cations cannot be as readily made[63] as $[Cp^*_2Sm(THF)_2][BPH_4]$, which is conveniently prepared from the divalent precursor $Cp^*_2Sm(THF)_2$.[26]

(58) Shannon, R. D. *Acta Crystallogr.* **1976**, *A32*, 751–767.
(59) Zinnen, H. A.; Pluth, J. J.; Evans, W. J. *J. Chem. Soc., Chem. Commun.* **1980**, 810–812.
(60) Atwood, J. L.; Hunter, W. E.; Wayda, A. L.; Evans, W. J. *Inorg. Chem.* **1981**, *20*, 4115–4119.
(61) Evans, W. J.; Sollberger, M. S.; Hanusa, T. P. *J. Am. Chem. Soc.* **1988**, *110*, 1841–1850.
(62) Rabe, G.; Roesky, H. W.; Stalke, D.; Power, F.; Sheldrick, G. M. *J. Organomet. Chem.* **1991**, *403*, 11–19.
(63) Bruno, J. W.; Hazin, P.; Schulte, G. K. *Organometallics* **1990**, *9*, 416–423.

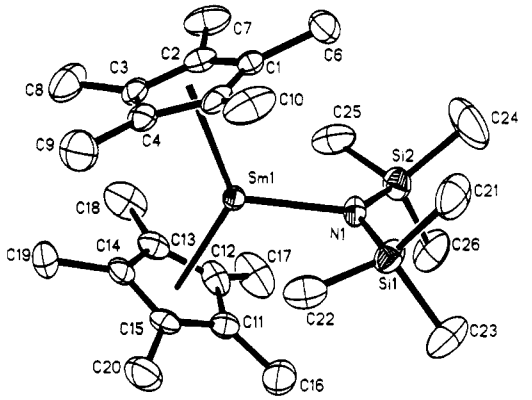

Figure 4. Molecular structure of $(C_5Me_5)_2Sm[N(SiMe_3)_2]$ (**8**), with probability ellipsoids drawn at the 50% level.

(c) $Cp^*_2Ln[N(SiMe_3)_2]$ Complexes as Precursors. (i) Synthesis. The best general route to $Cp^*_2Ln(C{\equiv}CPh)(THF)$ complexes involves the amide precursors $Cp^*_2Ln[N(SiMe_3)_2]$. These complexes are readily accessible Cp^*_2LnZ species which do not react with THF and are reactive enough under the appropriate conditions (see below) to metalate $HC{\equiv}CPh$.

Previous studies had shown that $Cp^*_2Y[N(SiMe_3)_2]$ could be cleanly made from $Cp^*_2YCl(THF)$ and $NaN(SiMe_3)_2$.[64] Apparently the steric bulk of the $N(SiMe_3)_2$ ligand was sufficient to prevent formation of undesirable NaCl adducts with metals the size of yttrium. $KN(SiMe_3)_2$ also gives alkali metal halide free products when it reacts with the KCl adducts of the larger, early lanthanide complexes $Cp^*_2LnCl_2K(THF)$, as shown in eq 18. These amide complexes were readily obtainable precursors and have proven to be useful reagents.

$$Cp^*_2LnCl_2K(THF) + KN(SiMe_3)_2 \rightarrow Cp^*_2Ln[N(SiMe_3)_2] + 2KCl \quad (18)$$
$$\mathbf{6\text{–}8}$$

$$Ln = Ce\ (\mathbf{6}),\ Nd\ (\mathbf{7}),\ Sm\ (\mathbf{8})$$

(ii) Structure. To fully characterize one of these early lanthanide amide complexes, an X-ray diffraction study of $Cp^*_2Sm[N(SiMe_3)_2]$ (**8**) was performed. Complex **8** is not isostructural with $Cp^*_2Y[N(SiMe_3)_2]$ (**23**),[64] although the complexes are very similar in many respects. The structure is shown in Figure 4, and selected bond distances and angles are given in Table III. The overall structures of the two molecules are similar in that (a) the (ring centroid)–Ln–(ring centroid) angles are comparable (132.2 and 132.4° for the two independent molecules in **23** and 132.8° for **8**), (b) the nitrogen atom in each complex is nearly coplanar (to within 0.05 Å) with both the Ln metal center and the two silicon atoms, (c) the two Me_3Si groups are eclipsed with respect to each other, and (d) the 2.750(15) Å Sm–C(Cp^*) average distance and the 2.301(3) Å Sm–N bond length in **8** are equivalent to the 2.682(4) and 2.678(4) Å Y–C(Cp^*) and 2.274(5) and 2.253(5) Å Y–N distances when the 0.06-Å difference in radial size is considered.[58]

Both molecules display some small N–Si–C angles in the 106–107° range (N(1)–Si(1)–C(22) and N(1)–Si(2)–C(25) in **8**). In **23**, these small angles were associated with short yttrium–methyl interactions, including one for which a 2.45(6) Å Y···H–CH_2–Si distance was observed. In **8**, the closest Sm···H–CH_2–Si distances for methyl groups involving C(22) and C(25) are 2.97 and 3.031 Å, respectively. These Sm···H distances are much more than 0.06 Å larger than the Y···H distances in **23**. Similarly, the more reliable Sm···C distances for the methyl groups exhibiting the small N-Si-C angles (Sm···C(22) = 3.216 Å and Sm···C(25) = 3.282 Å) are more than 0.06 Å longer than the analogous 2.970- and 3.181-Å distances in **23**. These Sm···C distances are also longer than the 2.972(9) and 2.952(9) Å Ce···C distances in $Cp^*Ce[N(SiMe_3)_2]_2$, which are also associated with small N–Si–C angles.[13a] Hence, although unusual angles are present in each of these complexes, this does not translate into analogously close metal···methyl distances in the samarium complex. This is rather unusual, since the larger metal center in **8** is sterically less saturated than that in **23** and might be expected to have more extensive agostic interactions. Too few analogous systems have been studied to decide if the longer Ln–N distance in the samarium complex prevents the closer approach of the methyl groups in that case.

Table III. Selected Interatomic Distances (Å) and Angles (deg) for $Cp^*_2Sm[N(SiMe_3)_2]$ (8)[a]

Sm(1)–Si(1)	3.387(1)	Sm(1)–C(15)	2.736(5)
Sm(1)–Si(2)	3.416(1)	Sm(1)–Cnt(1)	2.479
Sm(1)–N(1)	2.301(3)	Sm(1)–Cnt(2)	2.470
Sm(1)–C(1)	2.744(6)	Si(1)–N(1)	1.697(4)
Sm(1)–C(2)	2.733(6)	Si(1)–C(21)	1.875(6)
Sm(1)–C(3)	2.767(6)	Si(1)–C(22)	1.877(5)
Sm(1)–C(4)	2.767(6)	Si(1)–C(23)	1.878(8)
Sm(1)–C(5)	2.757(6)	Si(2)–N(1)	1.700(4)
Sm(1)–C(11)	2.769(6)	Si(2)–C(24)	1.865(7)
Sm(1)–C(12)	2.753(6)	Si(2)–C(25)	1.886(6)
Sm(1)–C(13)	2.736(5)	Si(2)–C(26)	1.873(9)
Sm(1)–C(14)	2.733(4)		
N(1)–Sm(1)–Cnt(1)	112.7	C(22)–Si(1)–C(23)	107.4(3)
N(1)–Sm(1)–Cnt(2)	114.5	N(1)–Si(2)–C(24)	115.1(3)
Cnt(1)–Sm(1)–Cnt(2)	132.8	N(1)–Si(2)–C(25)	106.4(2)
N(1)–Si(1)–C(21)	114.3(3)	C(24)–Si(2)–C(25)	106.5(3)
N(1)–Si(1)–C(22)	106.3(2)	N(1)–Si(2)–C(26)	114.0(3)
C(21)–Si(1)–C(22)	108.8(3)	C(24)–Si(2)–C(26)	105.8(3)
N(1)–Si(1)–C(23)	114.6(3)	C(25)–Si(2)–C(26)	108.6(3)
C(21)–Si(1)–C(23)	105.3(3)	Si(1)–N(1)–Si(2)	128.4(2)

[a] Cnt(1) is the centroid of the C(1)–C(5) ring; Cnt(2) is the centroid of the C(11)–C(15) ring.

(iii) Reactivity with $HC{\equiv}CPh$: Rate Acceleration in the Presence of a Coordinating Solvent. The $Cp^*_2Ln[N(SiMe_3)_2]$ complexes do not react with $HC{\equiv}CPh$ at temperatures up to 100 °C in toluene (eq 19). However, metalation does occur in THF (eq 20). This was somewhat

$$Cp^*_2Ln[N(SiMe_3)_2] + HC{\equiv}CPh \xrightarrow{\text{toluene}} \text{no reaction} \quad (19)$$

$$Cp^*_2Ln[N(SiMe_3)_2] + HC{\equiv}CPh \xrightarrow{THF} Cp^*_2Ln(C{\equiv}CPh)(THF) + HN(SiMe_3)_2 \quad (20)$$
$$\mathbf{2,\ 9,\ 10}$$

$$Ln = Ce\ (\mathbf{9}),\ Nd\ (\mathbf{10}),\ Sm\ (\mathbf{2})$$

surprising, since THF generally inhibits reactivity of organolanthanide complexes by filling the coordination sphere of the metal and blocking reaction sites.[48,65,66]

(64) den Haan, K. H.; de Boer, J. L.; Teuben, J. H.; Spek, A. L.; Kojic-Prodic, B.; Hays, G. R.; Huis, R. *Organometallics* **1986**, *5*, 1726.

(65) Evans, W. J.; Dominguez, R.; Hanusa, T. P. *Organometallics* **1986**, *5*, 263–270.

Equations 19 and 20 are obviously exceptions to this generalization.

Equation 20 provides a convenient general route to the $Cp^*_2Ln(C{\equiv}CPh)(THF)$ complexes. The cerium derivative **9** is bright red, the neodymium compound **10** is pale green, and the samarium complex **2** is bright yellow. Interestingly, not one of these complexes exhibits a strong $\nu_{C{\equiv}C}$ stretch in the IR spectrum. As expected, the complexes react readily with KC≡CPh to generate the $[Cp^*_2Ln(C{\equiv}CPh)_2K]_n$ compounds described above.

(d) Coupling Reactivity of $Cp^*_2Ce(C{\equiv}CPh)(THF)$ and $Cp^*_2Nd(C{\equiv}CPh)(THF)$. The THF-$d_8$ derivatives of $Cp^*_2Ce(C{\equiv}CPh)(THF)$ and $Cp^*_2Nd(C{\equiv}CPh)(THF)$ were heated in toluene in a reaction analogous to the samarium reaction (eq 5 above). After 16 h at 130 °C, a solution of the blue neodymium complex had assumed the dark red color also observed in the formation of the samarium trienediyl complex **1**. This is an unusual color for a neodymium complex. After 16 h at 100 °C, a solution of the bright red cerium complex similarly became dark red. The ^1H NMR spectra of these complexes showed that new products had been formed, but the broadened, shifted resonances were not structurally specific. Addition of THF to these solutions caused no obvious change. This is as expected if a butatrienediyl complex had formed, since **1** does not react with THF. Both the cerium and neodymium products were crystallographically characterized to unequivocally prove that coupling had occurred (eq 21), and the data showed them to be isostructural with $[Cp^*_2Sm]_2(\mu\text{-}\eta^2{:}\eta^2\text{-}PhC{=}C{=}C{=}CPh)$ (**1**).

$$2Cp^*_2Ln(C{\equiv}CPh)(THF) \xrightarrow[130\,^\circ C]{\text{toluene}} [Cp^*_2Ln]_2(\mu\text{-}\eta^2{:}\eta^2\text{-}PhC{=}C{=}C{=}CPh) + 2THF \quad (21)$$

11, 12

Ln = Ce (**11**), Nd (**12**)

Mechanistic Considerations. The fact that the alkynide coupling reaction could be achieved with both cerium and neodymium alkynides clearly demonstrated that an accessible divalent oxidation state was not required for the coupling reaction and that the reaction was not limited to samarium. Therefore, the problematic reaction scheme involving homolytic cleavage of the Ln—CCPh bond presented in eqs 6–8 was not reasonable. A more likely route by which the necessary Ln—CCPh cleavage is accomplished in this reaction is heterolytic cleavage, i.e. formal formation of $(PhC{\equiv}C)^-$ and a cationic lanthanide fragment. This is reasonable in terms of the properties of terminal alkynes which have strong H—CCR bonds but are relatively acidic. As mentioned earlier, the X-ray crystal structure of $Cp^*_2Sm(C{\equiv}CPh)(THF)$ revealed an unusually long Sm—CCPh distance, which could indicate that heterolytic Sm—CCPh cleavage might be favored in this complex.

A scheme incorporating heterolytic cleavage and the other data known on this coupling reaction is shown in Scheme II. The first step of the scheme is consistent with the kinetic data obtained for eq 5 (see above) and involves THF dissociation to form the reactive, formally seven-coordinate species "$Cp^*_2Ln(C{\equiv}CPh)$". The highly electrophilic metal center in this coordinatively unsaturated

Scheme II

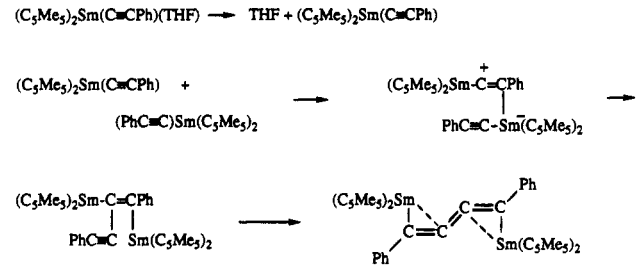

complex (see below) would ordinarily gain electron density by forming a bridged species with the α-carbon of an alkynide ligand of another $Cp^*_2Ln(C{\equiv}CPh)$ unit, as in the $[(C_5H_4R)_2Ln(\mu\text{-}C{\equiv}CR')]_2$ complexes (R = H, Me, CMe_3; R′ = CMe_3, Ph; Ln = Sm, Er).[42,43,60] If this is prevented by the steric constraints of the four pentamethylcyclopentadienyl ligands, the lanthanide center may instead interact with the electron density of the C≡C bond and/or with the β-carbon of the alkynide ligand. The latter interaction has precedent in organotransition-metal chemistry, e.g., eq 22.[67,68] In this case, attack of an electrophile

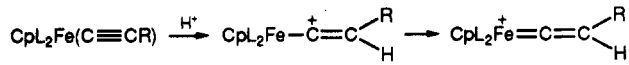

(22)

at the β-alkynide position generates a positive charge at the α-carbon. With transition metals, this positive charge is neutralized by formal oxidation of the metal and formation of a carbene complex. In the lanthanide case, this oxidation is not possible and the positively charged α-carbon must find electron density elsewhere. If the electron density is obtained from the Ln—CCPh bond of another "$Cp^*_2Ln(C{\equiv}CPh)$" unit, i.e., if heterolytic Ln—CCPh bond cleavage occurs, the crucial C–C bond-forming step in the coupling reaction is accomplished. The last step in the scheme involves movement of the Cp^*_2Ln moieties to their preferred orientation around the newly formed $(PhCCCCPh)^{2-}$ ion.

Effect of the R Group. Scheme II could be tested by varying the alkynide substituent. Alkynide complexes derived from less acidic alkynes would be less prone to heterolytic cleavage and would not be expected to couple as readily via this route. Coupling could also be inhibited by sterically bulky substituents.

(a) Synthesis and Reactivity of $Cp^*_2Sm(C{\equiv}CR')(THF)$ Complexes (R′ = CH_2CH_2Ph (13), CH_2NEt_2 (14), $CH_2CH_2CHMe_2$ (15), $CHMe_2$ (16), CMe_3 (24)[26]). The five alkynide complexes identified in eq 23 were readily prepared from the divalent $Cp^*_2Sm(THF)$ and the appropriate alkyne. These THF-solvated alkynide com-

$$Cp^*_2Sm(THF) + HC{\equiv}CR' \xrightarrow{\text{toluene}} Cp^*_2Sm(C{\equiv}CR')(THF) \quad (23)$$

13–16, 24

R′ = CH_2CH_2Ph (**13**), CH_2NEt_2 (**14**), $CH_2CH_2CHMe_2$ (**15**), $CHMe_2$ (**16**), CMe_3 (**24**)

plexes could also be prepared from $Cp^*_2Sm[N(SiMe_3)_2]$,

(66) Schumann, H.; Palamidis, E.; Loebel, J. *J. Organomet. Chem.* **1990**, *384*, C49–C52.

(67) Davison, A.; Selegue, P. *J. Am. Chem. Soc.* **1980**, *102*, 2455–2456.

(68) Bruce, M. I.; Swincon, A. G. *Adv. Organomet. Chem.* **1983**, *22*, 65–67.

but the divalent route provided a faster route to a cleaner product. For (2-pyridyl)C≡CH, reaction 23 did not proceed to a single product and the desired alkynide complex was not separated from the brown reaction mixture. Reactivity with the pyridyl group is a likely complication with this alkyne.[53,69]

By the procedure successful for the coupling of $Cp^*_2Sm(C{\equiv}CPh)(THF)$ as shown in eq 5, the five alkynide complexes **13–16** and **24** were heated in toluene-d_8 in sealed NMR tubes. Even with forcing conditions of temperatures as high as 140 °C for 2 days, no reaction was observed for any of these alkynide complexes (eq 24). This implied that there was something special about the phenyl substituent in $(C_5Me_5)_2Sm(C{\equiv}CPh)(THF)$ in regard to the coupling reaction.

$$\underset{\textbf{13–16, 24}}{Cp^*_2Sm(C{\equiv}CR')(THF)} \xrightarrow[140°C]{\text{toluene}} \text{no reaction} \quad (24)$$

(b) Formation of THF-Free "$Cp^*_2Sm(C{\equiv}CR)$" Moieties Using $[Cp^*_2Sm(\mu\text{-}H)]_2$ as a Precursor. (i) Reactivity. Since THF dissociation appears to be the crucial step in the coupling of $Cp^*_2Sm(C{\equiv}CPh)(THF)$, formation of "$Cp^*_2Sm(C{\equiv}CR)$" moieties in the absence of THF was pursued by reacting alkynes with $[Cp^*_2Sm(\mu\text{-}H)]_2$ according to eq 3. The reactions of $R'C{\equiv}CH$ with $[Cp^*_2Sm(\mu\text{-}H)]_2$ were fast, as evidenced by immediate gas evolution (presumably hydrogen) and by rapid color changes from orange to brown. However, in contrast to the reaction with $PhC{\equiv}CH$, which formed trienediyl **1** quantitatively, the reactions with the other alkynes gave mixtures of products. Attempts to obtain simpler product distributions by varying the solvent, the temperature, and the ratio of the starting materials were unsuccessful. However, in the case of $HC{\equiv}CCMe_3$, two products were isolated from the reaction mixture as crystalline materials (eq 25) and were identifiable by X-ray crystallography as described below.

$$[Cp^*_2Sm(\mu\text{-}H)]_2 + HC{\equiv}CCMe_3 \rightarrow \underset{\textbf{17}}{[Cp^*_2Sm(C{\equiv}CCMe_3)]_2} + \underset{\textbf{18}}{Cp^*_2Sm[Me_3CCH{=}CC(CMe_3){=}CH_2]} \quad (25)$$

(ii) Isolation of the Unsolvated, Uncoupled Alkynide Complex $[Cp^*_2Sm(C{\equiv}CCMe_3)]_2$ (17). The yellow crystals obtained by crystallization of the $[Cp^*_2Sm(\mu\text{-}H)]_2/HC{\equiv}CCMe_3$ reaction mixture from toluene were identified as the unsolvated, uncoupled alkynide $[Cp^*_2Sm(C{\equiv}CCMe_3)]_2$ (**17**), shown in Figures 5 and 6. The fact that an uncoupled *tert*-butyl alkynide complex is isolated is consistent with Scheme II. The *tert*-butyl alkynide complex is expected to be less prone to heterolytic cleavage than a Sm—CCPh complex due to the electron-donating nature of CMe_3 *vs* Ph and due to the steric bulk of the CMe_3 group. The solid-state structure of **17** described below further supports Scheme II.

Examination of one monometallic unit of **17** (Figure 5) shows considerable asymmetry in the location of the alkynide ligand. If the alkynide ligand were located symmetrically, the two ring centroids and the α-carbon of the alkynide would be rigorously trigonal planar and the samarium atom would lie in this plane. In **17**, the samarium atom lies 0.38 Å out of this plane.[70]

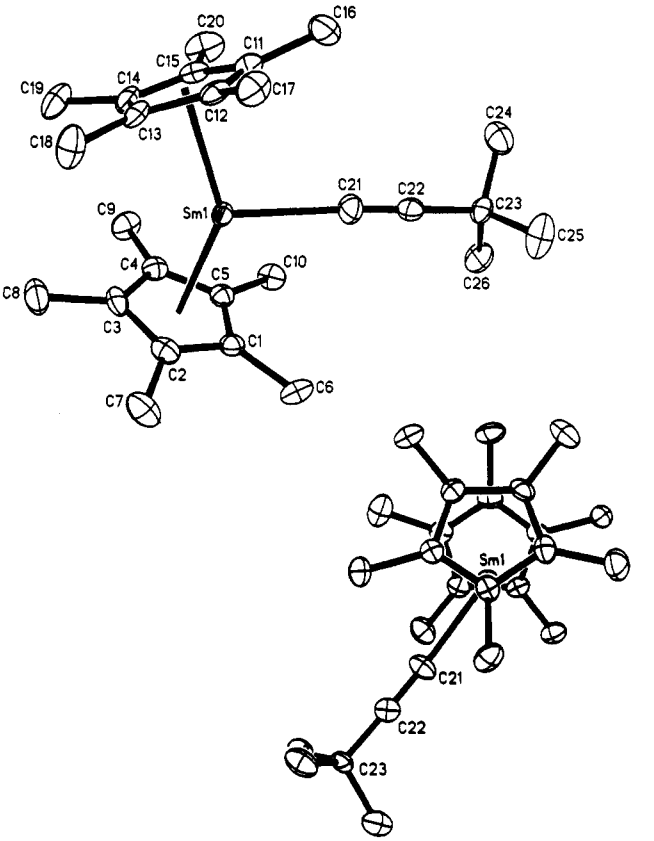

Figure 5. Molecular structure of one $(C_5Me_5)_2Sm(C{\equiv}CCMe_3)$ unit of **17**, with probability ellipsoids drawn at the 50% level (a) side view; (b) top view.

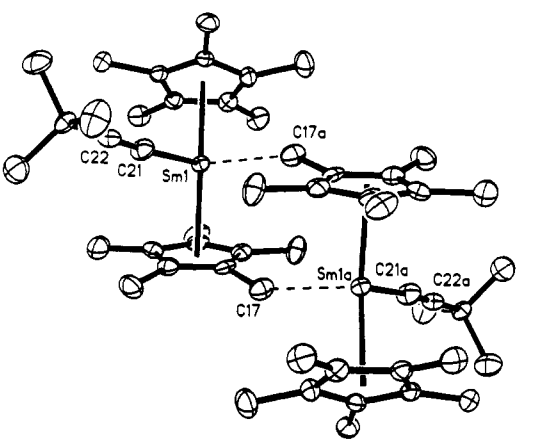

Figure 6. Molecular structure of $[(C_5Me_5)_2Sm(C{\equiv}CCMe_3)]_2$ (**17**), with probability ellipsoids drawn at the 50% level.

The observed asymmetry in the monometallic unit can be rationalized as due to a long-distance intermolecular interaction between adjacent pairs of monometallic units. As shown in Figure 6, a methyl carbon atom of a Cp* ring of the adjacent molecule points directly at the open area

(69) Evans, W. J.; Chamberlain, L. R. Unpublished results.

(70) Alternatively, this asymmetry can be described by how far the α-carbon atom lies out of the plane defined by samarium and the two ring centroids. In **17**, the α-carbon lies 1.42 Å out of this plane. Asymmetry of this type has previously been observed in the divalent complexes $Cp^*_2Sm(ether)$ (ether = THF, tetrahydropyran).[71] In those cases the samarium atoms were 0.42 and 0.34 Å, respectively, out of the plane defined by the two ring centroids and the oxygen donor atoms.

(71) (a) Evans, W. J.; Ulibarri, T. A. *Polyhedron* **1989**, *8*, 1007–1014. (b) Evans, W. J.; Kociok-Kohn, G.; Foster, S. E.; Ziller, J. W.; Doedens, R. J. *J. Organomet. Chem.* **1993**, *444*, 61–66.

Table IV. Selected Interatomic Distances (Å) and Angles (deg) for $[Cp^*_2Sm(C{\equiv}CCMe_3)]_2$ (17)[a]

Sm(1)–C(1)	2.685(5)	Sm(2)–C(27)	2.738(5)
Sm(1)–C(2)	2.714(6)	Sm(2)–C(28)	2.696(6)
Sm(1)–C(3)	2.719(5)	Sm(2)–C(29)	2.696(5)
Sm(1)–C(4)	2.694(4)	Sm(2)–C(30)	2.702(6)
Sm(1)–C(5)	2.677(4)	Sm(2)–C(31)	2.735(6)
Sm(1)–C(11)	2.743(6)	Sm(2)–C(37)	2.690(6)
Sm(1)–C(12)	2.711(4)	Sm(2)–C(38)	2.701(7)
Sm(1)–C(13)	2.689(5)	Sm(2)–C(39)	2.700(6)
Sm(1)–C(14)	2.691(6)	Sm(2)–C(40)	2.707(5)
Sm(1)–C(15)	2.697(7)	Sm(2)–C(41)	2.694(5)
Sm(1)–C(21)	2.419(6)	Sm(2)–C(47)	2.403(6)
Sm(1)–C(17A)	3.006(7)	Sm(2)–C(36A)	3.039(6)
C(21)–C(22)	1.209(8)	C(47)–C(48)	1.207(8)
C(22)–C(23)	1.484(8)	C(48)–C(49)	1.465(8)
C(21)–Sm(1)–Cnt(1)	105.6	C(47)–Sm(2)–Cnt(3)	105.4
C(21)–Sm(1)–Cnt(2)	106.8	C(47)–Sm(2)–Cnt(4)	104.2
Cnt(1)–Sm(1)–Cnt(2)	139.5	Cnt(3)–Sm(2)–Cnt(4)	142.3
Sm(1)–C(21)–C(22)	174.7(4)	Sm(2)–C(47)–C(48)	166.1(6)
C(21)–C(22)–C(23)	178.5(5)	C(47)–C(48)–C(49)	178.8(7)

[a] Cnt(1) is the centroid of the C(1)–C(5) ring; Cnt(2) is the centroid of the C(11)–C(15) ring; Cnt(3) is the centroid of the C(27)–C(31) ring; Cnt(4) is the centroid of the C(37)–C(41) ring.

around the metal. Such long-distance interactions between lanthanides and other atoms have been evaluated in the past by comparing these distances to the metal–C(Cp*) distance in the complex.[23] In complexes which have Ln···C distances similar to the Ln–C(C_5Me_5) average or less than the longest Ln–C(Cp*) distances, the unconventional Ln···C interactions appear to be significant. The 2.773-Å Sm···o-C distance in the styrene complex $[Cp^*_2Sm]_2(PhCHCH_2)$ is such an example.[23] Complexes with interactions 0.1–0.2 Å greater than the Ln–C(Cp*) distance are known and show almost no perturbation in the distant ligand; i.e., these interactions are weak. Examples include $Cp^*_2Yb(MeC{\equiv}CMe)$,[72] $Cp^*_2Yb(H_2C{=}CH_2)Pt(PPh_3)$,[73] $Cp^*_2Yb(\mu\text{-}Me)BeCp^*$,[74] and $[Cp^*_2Sm]_2(\mu\text{-}C_5H_5)$.[75] Since the 3.006(7) Å Sm–C(Me′) distance in **17** is 0.3 Å greater than the 2.702(19) Å Sm–C(Cp*) average (Table IV) the intermolecular interactions in **17** must be considered weak by this analysis.

Although the Sm–C(Me′) distance in **17** is long compared to the average Sm–C(Cp*) distance, it is apparently long enough to cause the asymmetry in the alkynide ligand location. This structural feature is consistent with Scheme II in that it shows that a seven-coordinate $Cp^*_2Sm(C{\equiv}CR)$ complex is so electrophilic that it will seek electron density from a donor as weak as a Cp* methyl group.

The 2.419(6) Å Sm–C(alkynide) distance in **17** is in the normal range, considering that Ln–CCR bonds are usually 0.05 Å shorter than Ln–C(alkyl) bonds[42] and eight-coordinate $Cp^*_2SmMe(THF)$[27] has a Sm–C(Me) distance of 2.48(1) Å. The Sm–C(alkynide) distance in **17** is comparable to the analogous 2.49(2) Å distance in eight-coordinate $Cp^*_2Sm(C{\equiv}CPh)(THF)$[26] within the error limits, but the distance in the latter complex was analyzed to be unusually long.

The 1.209(8) Å C≡C bond distance in **17** is in the normal 1.188(8)–1.29(5) Å range of distances found in early-

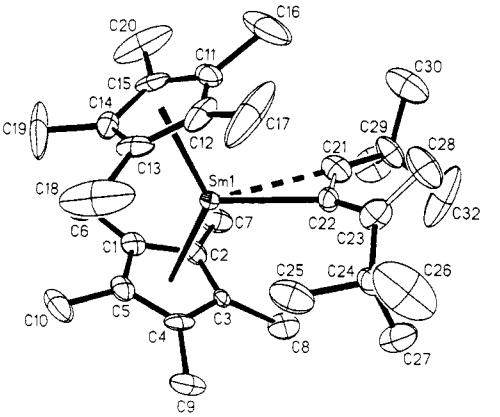

Figure 7. Molecular structure of $(C_5Me_5)_2Sm[Me_3CCH{=}CC(CMe_3){=}CH_2]$ (**18**), with probability ellipsoids drawn at the 30% level.

Table V. Interatomic Distances (Å) and Angles (deg) for $Cp^*_2Sm[Me_3CCH{=}CC(CMe_3){=}CH_2]$ (18)

Sm(1)–C(1)	2.769(12)	Sm(1)–C(15)	2.686(14)
Sm(1)–C(2)	2.734(12)	Sm(1)–C(21)	2.902(14)
Sm(1)–C(3)	2.727(11)	Sm(1)–C(22)	2.455(12)
Sm(1)–C(4)	2.734(12)	C(21)–C(22)	1.356(18)
Sm(1)–C(5)	2.767(12)	C(21)–C(29)	1.489(21)
Sm(1)–C(11)	2.712(16)	C(22)–C(23)	1.432(18)
Sm(1)–C(12)	2.742(15)	C(23)–C(24)	1.470(20)
Sm(1)–C(13)	2.724(15)	C(23)–C(28)	1.407(23)
Sm(1)–C(14)	2.680(12)		
C(21)–Sm(1)–C(22)	27.8(4)	Sm(1)–C(22)–C(23)	133.3(9)
Sm(1)–C(21)–C(22)	57.4(7)	C(21)–C(22)–C(23)	130.7(12)
Sm(1)–C(21)–C(29)	166.8(9)	C(22)–C(23)–C(24)	118.6(12)
C(22)–C(21)–C(29)	135.1(13)	C(22)–C(23)–C(28)	126.1(14)
Sm(1)–C(22)–C(21)	94.8(8)	C(24)–C(23)–C(28)	114.6(13)

transition-metal and lanthanide alkynide complexes.[26] This distance is longer than the 1.12(2) Å average distance found in $Cp^*_2Sm(C{\equiv}CPh)(THF)$ (**2**),[26] a distance which is more typical of alkali-metal alkynides.[26] Hence, we find that the samarium alkynide with a short C–C distance and a long Sm–C distance (i.e. **2**) couples more readily than the complex with more normal Sm–C and C–C distances (i.e. **17**).

(iii) Butadienyl Byproduct of the $[Cp^*_2Sm(\mu\text{-}H)]_2$/HC≡CCMe$_3$ Reaction. The orange crystals isolated from the $[Cp^*_2Sm(\mu\text{-}H)]_2$/HC≡CCMe$_3$ reaction mixture were identified as the compound $Cp^*_2Sm[Me_3CCH{=}CC(CMe_3){=}CH_2]$ (**18**). The structure of **18** is shown in Figure 7, and selected bond distances and angles are given in Table V. **18** is formally comprised of one Cp^*_2SmH unit and two molecules of HC≡CCMe$_3$. The ligand that is formed by these three molecules can be formally viewed as a 1,3-di-*tert*-butyl-1,3-butadiene metalated at the 2-position:

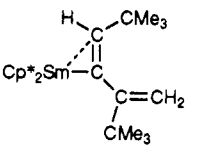

The C(21)–C(22) and C(23)–C(28) distances (1.356(18) and 1.407(23) Å, respectively) are consistent with this. The 2.455(12) Å Sm–C(22) distance is similar to the 2.484(14) Å Sm–C(Me) distance in $Cp^*_2SmMe(THF)$,[27] and the 2.72(5) Å average Sm–C(Cp*) distance is within the normal range. The 2.902(14) Å Sm–C(21) distance is too long for a significant interaction, using the criteria discussed above for **17**.

(72) Burns, C. J.; Andersen, R. A. *J. Am. Chem. Soc.* **1987**, *109*, 941–942.
(73) Burns, C. J.; Andersen, R. A. *J. Am. Chem. Soc.* **1987**, *109*, 915–917.
(74) Burns, C. J.; Andersen, R. A. *J. Am. Chem. Soc.* **1987**, *109*, 5853–5855.
(75) Evans, W. J.; Ulibarri, T. A. *J. Am. Chem. Soc.* **1987**, *109*, 4292–4297.

The composition of 18 can be explained by insertion of one molecule of alkyne into the samarium–hydride bond to make an alkenyl complex followed by insertion of another molecule of alkyne into the samarium–alkenyl bond. Insertion of alkynes into the bonds of lanthanide and yttrium with hydride and alkyl groups is well precedented,[48,57,76] although metalation of internal alkynes has also been observed.[57] Recently, Teuben and coworkers have demonstrated how insertion of alkynes into yttrium- and lanthanide–alkyl bonds can generate catalytic cycles leading to cyclodimerization of alkynes.[48,57]

However, the regiochemistry of the formation of 18 is not so easily understood. The sterically most favorable way for successive RC≡CH alkyne insertions into a Sm—H bond to occur is to form a Sm—CH=CHR unit first and then a Sm—CH=C(R)—CH=CHR moiety. In both cases, the new metal–carbon bond forms at the sterically least crowded, hydrogen-substituted end of the alkyne.[48] With $Me_3CC{\equiv}CH$, this pattern of insertions generates a 1,3-di-*tert*-butyl-*4*-[Cp^*_2Sm]-butadiene, not the 1,3-di-*tert*-butyl-2-[Cp^*_2Sm]-butadiene observed in 18. In fact, there is no combination of two alkyne insertions, regardless of the steric preferences, which leads to the observed product. Substituent migration, β-hydrogen elimination, and reinsertion with isomerization, or some intermolecular metalation, must occur to give the observed product. Unfortunately, since 18 is only a minor product of this reaction, more detailed information on its formation was not available. Attempts to make 18 directly from Cp^*_2Sm,[77] $Me_3CC{\equiv}CH$, and $Me_3CCH{=}CH_2$ were not successful.

(c) Formation of THF-Free "$Cp^*_2Sm(C{\equiv}CR)$" Moieties using Cp^*_2Sm as a Precursor. (i) Reaction Chemistry. An alternative route to THF-free alkynide complexes involved the reaction of Cp^*_2Sm[77] with alkynes according to eq 4. Reacting stoichiometric amounts of $HC{\equiv}CCH_2CH_2Ph$, $HC{\equiv}CCH_2CH_2CHMe_2$, and $HC{\equiv}CCHMe_2$ with Cp^*_2Sm at −78 °C gave single products. With the first two alkynes, the solution had turned the dark red color of 1 by the time the reaction mixture had been warmed to room temperature. With $HC{\equiv}CCHMe_2$, the reaction mixture remained dark brown for a number of hours and only after remaining at room temperature overnight did the solution turn dark red. The dark red color of these products plus the fact that addition of THF to each of these complexes failed to form the solvated alkynide species, $Cp^*_2Sm(C{\equiv}CR)(THF)$, suggested that coupling had occurred.

The ^1H NMR spectrum of the $PhCH_2CH_2C{\equiv}CH$ reaction product 19 had two highly shifted resonances at −12.94 and −1.48 ppm with integrals appropriate for methylene groups. In contrast, the methylene groups in $Cp^*_2Sm(C{\equiv}CCH_2CH_2Ph)(THF)$ were found at 3.34 and 3.47 ppm. The shifted resonances suggested that these methylene groups were interacting with the paramagnetic samarium center. To probe this further and to establish the identity of this reaction product, the complex was characterized by X-ray crystallography.

The X-ray crystal structure determination on 19 established that a coupling reaction had occurred in the $HC{\equiv}CCH_2CH_2Ph$ reaction and that a trienediyl complex,

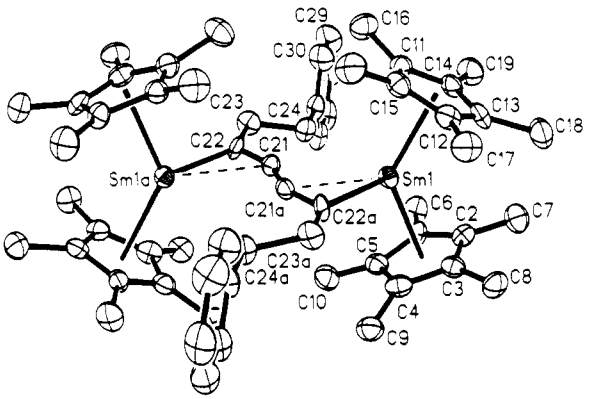

Figure 8. Molecular structure of $(C_5Me_5)_2Sm[\mu\text{-}\eta^2{:}\eta^2\text{-}PhCH_2CH_2C{=}C{=}C{=}CCH_2CH_2Ph]$ (19), with probability ellipsoids drawn at the 50% level.

$[Cp^*_2Sm]_2(\mu\text{-}\eta^2{:}\eta^2\text{-}PhCH_2CH_2C{=}C{=}C{=}CCH_2CH_2Ph)$, had been formed (Figure 8 and eq 26). Formation of a

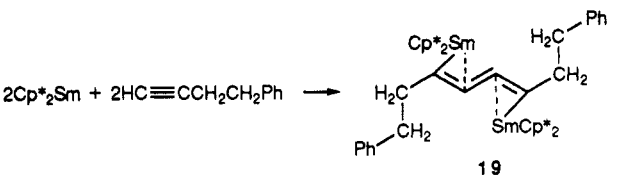

(26)

trienediyl ligand from $HC{\equiv}CCH_2CH_2Ph$ indicated that alkyl- as well as phenyl-substituted alkynides could participate in this lanthanide-based C–C bond formation reaction. However, the $HC{\equiv}CCH_2CH_2Ph$ system did still contain a phenyl ring which could be involved in assembling some bimetallic precoupling intermediate. Hence, it was desirable to investigate a case in which no phenyl groups were present. Therefore, crystallographic data were also obtained on the $HC{\equiv}CCH_2CH_2CHMe_2$ reaction product 20. Although only the connectivity of the atoms in this complex was established by the crystallographic data, it was determined that coupling had occurred and another example of a trienediyl complex in which two of the methylene groups are oriented toward the samarium centers was found (eq 27). The ^1H NMR spectrum of 20, like that of 19, has shifted resonances assignable to methylene groups at −12.35 and −2.17 ppm.

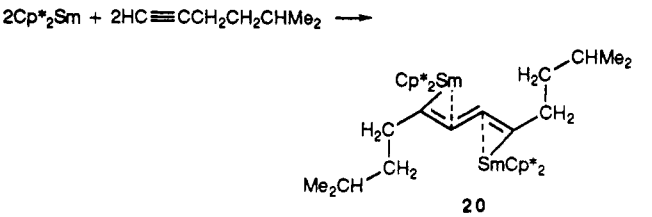

(27)

Structural data have not yet been obtained on the $HC{\equiv}CCHMe_2$ reaction product. Like 19 and 20, it has highly shifted resonances in its ^1H NMR spectrum and a similar structure seems likely.

(ii) Structure of a Coupled Product Which Contains Agostic Interactions. Comparison of the structure of 19 (Table VI) to those of the trienediyl complexes previously characterized by X-ray diffraction, $[Cp^*_2Sm]_2(\mu\text{-}\eta^2{:}\eta^2\text{-}PhC{=}C{=}C{=}CPh)\cdot 2MeC_6H_5$ (1a)[16] and $[Cp^*_2Sm]_2(\mu\text{-}\eta^2{:}\eta^2\text{-}PhC{=}C{=}C{=}CPh)\cdot 2C_6H_6$ (1b)[14] shows that there can be considerable variation in the metrical parameters of organosamarium complexes of this type of ligand. A

(76) Evans, W. J.; Meadows, J. H.; Hunter, W. E.; Atwood, J. L. *J. Am. Chem. Soc.* **1984**, *106*, 1291–1300.

(77) Evans, W. J.; Hughes, L. A.; Hanusa, T. P. *Organometallics* **1986**, *5*, 1285–1291.

Table VI. Interatomic Distances (Å) and Angles (deg) for $[Cp^*_2Sm]_2[\mu\text{-}\eta^2\text{:}\eta^2\text{-}PhCH_2CH_2C{\equiv}C{-}C{\equiv}CCH_2CH_2Ph]$ (19)

Sm(1)–C(1)	2.727(8)	Sm(1)–C(15)	2.737(8)
Sm(1)–C(2)	2.754(7)	Sm(1)–C(21)	2.909(6)
Sm(1)–C(3)	2.709(8)	Sm(1)–C(21A)	2.689(6)
Sm(1)–C(4)	2.714(8)	Sm(1)–C(22A)	2.483(7)
Sm(1)–C(5)	2.727(8)	Sm(1)–C(24)	3.748
Sm(1)–C(11)	2.736(8)	C(21)–C(22)	1.286(11)
Sm(1)–C(12)	2.698(8)	C(21)–C(21A)	1.353(17)
Sm(1)–C(13)	2.742(7)	C(22)–C(23)	1.518(12)
Sm(1)–C(14)	2.746(7)		

C(21)–Sm(1)–C(21A)	27.6(3)	C(22)–C(21)–C(21A)	152.1(8)
C(21)–Sm(1)–C(22A)	56.1(2)	Sm(1A)–C(21)–C(21A)	85.3(5)
C(21A)–Sm(1)–C(22A)	28.4(3)	C(21)–C(22)–C(23)	126.1(6)
Sm(1)–C(21)–C(22)	140.8(5)	C(21)–C(22)–Sm(1A)	84.7(5)
C(22)–C(21)–Sm(1A)	66.8(4)	C(23)–C(22)–Sm(1A)	149.1(5)
Sm(1)–C(21)–C(21A)	67.1(5)		

Table VII. Summary of Distances (Å) and Angles (deg) for the Trienediyls $[(C_5Me_5)_2Sm]_2[\mu\text{-}\eta^2\text{:}\eta^2\text{-}PhCH_2CH_2C{\equiv}C{-}C{\equiv}CCH_2CH_2Ph]$ (19), $[(C_5Me_5)_2Sm]_2(\mu\text{-}\eta^2\text{:}\eta^2\text{-}PhC{\equiv}C{-}C{\equiv}CPh)\cdot 2MeC_6H_5$ (1a),[16] and $[(C_5Me_5)_2Sm]_2(\mu\text{-}\eta^2\text{:}\eta^2\text{-}PhC{\equiv}C{-}C{\equiv}CPh)\cdot 2C_6H_6$ (1b)[14]

	19	1a	1b
C(21a)–C(21)–C(22)	152.2(8)	154(1)	146.9(10)
C(21)–C(22)–C(23)	126.1(6)	125(1)	123.7(10)
Cnt–Sm–Cnt	132.2	133.9	133.7
Sm–C(ring) av	2.73	2.71	2.71
Sm–C(22a)	2.483(7)	2.48(1)	2.505(9)
C(21a)–C(21)	1.353(17)	1.29(2)	1.298(19)
C(21)–C(22)	1.286(11)	1.33(2)	1.363(17)
Sm–C(21a)	2.689(6)	2.76(1)	2.807(8)
Sm–C(21)	2.909(6)	3.03(1)	2.963(9)

comparison of the metrical data is summarized in Table VII and discussed below.

There are many similarities among **19**, **1a**, and **1b**, including the coplanarity of the samarium centers with the carbon atoms of the butatriene fragment, the C(21a)–C(21)–C(22) angles, the C(21)–C(22)–C(23) angles, the Cnt–Sm–Cnt (Cnt = ring centroid) angles, the average Cnt–Sm–Cnt distances, and the Sm(1)–C(22a) distances. However, structural differences among these compounds include the following: the Cp* rings are staggered in **19** whereas they are eclipsed in **1a** and **1b**, the central C=C bond length of the butatriene fragment is significantly longer in **19** than in **1a** and **1b**, the terminal C=C bond lengths of the butatriene fragment are significantly shorter in **19** than in **1a** and **1b**, and the distances of the samarium atoms to the two central carbon atoms of the butatriene fragment are significantly shorter in **19** than in **1a** and **1b**. Apparently the degree of interaction of the samarium centers in these complexes with the double bonds of the trienediyl is variable and this can affect the C=C bond distances. The other main difference in **19** is that C(24) is directed toward the samarium center. The Sm(1)–C(24) distance of 3.748 Å is very long, but the angular orientation and the shifted NMR signals are consistent with an agostic interaction between this CH_2 group and the metal. Consistent with a weak interaction, little difference is seen between the Cnt–Sm–Cnt angles and the average Sm–C(ring) distances among **19**, **1a**, and **1b**. It is interesting to note how substantially this very long distance interaction affects the ^1H NMR resonances.

Steric and Electronic Effects of the Alkynide Substituent on Coupling. The results described above indicate that a combination of steric and electronic factors determine if C–C bond formation will occur between alkynide ligands in organolanthanide complexes. Clearly, if steric crowding is minimal in bis(cyclopentadienyl)lanthanide alkynides, simple bridged dimers will form. The evidence for this is the crystallographic data on $[(C_5H_5)_2Er(\mu\text{-}C{\equiv}CCMe_3)]_2$,[60] $[(C_5H_4Me)_2Sm(\mu\text{-}C{\equiv}CCMe_3)]_2$,[42] and $[(C_5H_4CMe_3)_2Sm(\mu\text{-}C{\equiv}CPh)]_2$.[43] For pentamethylcyclopentadienyl complexes, such bridged dimers are likely to be too sterically crowded to form. Therefore, when $Cp^*_2Ln(C{\equiv}CR)$ moieties are generated, they must achieve steric saturation in some other way. The solid-state structure of $[Cp^*_2Sm(C{\equiv}CCMe_3)]_2$ (**17**) indicates that some $Cp^*_2Ln(C{\equiv}CR)$ complexes are unable to form simple alkynide-bridged dimers, but they are so sterically unsaturated that they will interact with a methyl group of a Cp* ring. Comparison of "$Cp^*_2Sm(C{\equiv}CCMe_3)$" and "$Cp^*_2Sm(C{\equiv}CCPh)$" suggests that if a $Cp^*_2Sm(C{\equiv}CR)$ unit can readily undergo heterolytic cleavage of the Sm–C bond, C–C coupling can provide a route to eight-coordinate metal centers by forming trienediyl complexes such as **1**. This correlation of coupling reactivity with capacity for heterolytic cleavage, i.e., with the acidity of the parent alkyne, is not as simple as phenyl vs alkyl, because the alkyl-substituted alkynides $PhCH_2CH_2C{\equiv}C$, $Me_2CHCH_2CH_2C{\equiv}C$, and $Me_2CHC{\equiv}C$ also undergo coupling. Comparison of these alkyl-substituted alkynides with $Me_3CC{\equiv}C$ suggests that when the alkyl substituent is bulky enough, coupling can be prevented. Hence, the ideal system for lanthanide-based alkynide coupling is one in which the alkyne substituent is neither too sterically bulky nor too electron donating.

Removal of the Trienediyl Ligand. Cyclic Formation of Enyne from Alkynes. To determine if the $(PhC{\equiv}C{-}C{\equiv}CPh)^{2-}$ ligand formed in the above reactions could be removed from the samarium centers as a butatriene, the reactivity of **1** with $PhC{\equiv}CH$ was examined. This reagent was chosen since it could give provide a cyclic reaction for converting alkynes to cumulenes.

Initial reactivity studies in toluene showed no reaction between **1** and $PhC{\equiv}CH$ up to temperatures of 110 °C with up to a 100-fold excess of alkyne. However, in THF the reaction of 2 equiv of $PhC{\equiv}CH$ with **1** gives an immediate color change from dark red to bright yellow within 5 min. NMR spectroscopy indicated that the desired $Cp^*_2Sm(C{\equiv}CPh)(THF)$ (**2**) was a product of this reaction. Sublimation of the reaction mixture at 80 °C and 10^{-5} Torr separated another product, 1,4-diphenyl-1(*E*)-buten-3-yne, which was identified by NMR, IR, and GC/MS analysis. Hence, the rearranged product $PhCH{=}CHC{\equiv}CPh$ is isolated from this reaction instead of the cumulene $PhCH{=}C{=}C{=}CHPh$. The overall reaction is shown in eq 28. Because **2** is regenerated in this reaction,

$$\underset{\mathbf{1}}{[Cp^*_2Sm]_2[\mu\text{-}\eta^2\text{:}\eta^2\text{-}PhC{=}C{=}C{=}CPh]} + 2PhC{\equiv}CH \rightarrow \underset{\mathbf{2}}{Cp^*_2Sm(C{\equiv}CPh)(THF)} + PhCH{=}CHC{\equiv}CPh \quad (28)$$

a two-step cycle by which $PhC{\equiv}CH$ can be converted to an enzyme by a tail-to-tail terminal alkyne coupling is obtained. Two complete cycles were performed on a sample of **1** without decomposition of the organosamarium species to demonstrate the cyclic nature of this process (Scheme I). In contrast, reaction of $Cp^*_2Y[CH(SiMe_3)_2]$ with $PhC{\equiv}CH$ gives predominantly a head-to-tail dimer, whereas with larger metals $Cp^*_2Ln[CH(SiMe_3)_2]$ (Ln =

La, Ce) gives a mixture with the tail-to-tail dimer dominating.[48] As discussed previously,[48] a complicated mixture of steric and electronic factors apparently lead to the product variations observed in lanthanide-based alkyne oligomerizations. The diversity of the results suggests that careful adjustment of the specific metal–ligand combination may provide precise control of such processes.

Conclusion

The results described above show that lanthanide-based hydrocarbyl *ligand* coupling reactions can now be considered as part of the reaction chemistry available for exploitation with organolanthanide complexes. The C–C bond formation reactivity described here demonstrates that, under the appropriate conditions, hydrocarbyl ligands attached to lanthanides can be coupled in reactions formally equivalent to C–C bond formation in transition-metal-based reductive eliminations (cf. eqs 6–8). Mechanistically, the reactions are very different. The lanthanide-based coupling does not require a change in oxidation state, and the experimental observations imply that the reactivity is driven by the electrophilicity of the metal center.

These results force a reassessment of the previous view of the reactivity of organolanthanide complexes. Clearly, with the appropriate manipulation of steric factors, conditions can be generated in which ligands previously not expected to be able to combine can couple in a very facile, energetically accessible reaction. Through steric control, the electrostatic barriers can be circumvented. These results also show that reactions which fail in noncoordinating solvents can sometimes be achieved in coordinating media. Evidently, the former expectation that coordinating solvents will inhibit the reactivity of the electrophilic organolanthanides must be evaluated on a case-by-case basis.

These results provide another example of exceptional organolanthanide chemistry which results as a consequence of the presence of the preferred tetrahedral orientation of four Cp* rings in a bimetallic complex.[41] In this case, the tetrakis(cyclopentadienyl) environment blocks simple dimer formation and leads to the coupling reactivity. The effects of this type of bimetallic coordination chemistry must always be considered in reactions of bis(pentamethylcyclopentadienyl)lanthanide complexes.

Finally, this research suggests that there are likely to be other reactions which ordinarily are not expected for organolanthanides but which can be achieved by developing special ligand sets. As predicted earlier,[78] with the appropriate ligand environment, a wide reaction chemistry is available to these metals. This generalization should be extended from monometallic systems to bi- and polymetallic complexes, and approaches to new reactions should include the use of steric factors to prevent the normal result, while generating a reactive metal center which must do unusual chemistry to achieve a more favorable ligand environment.

Acknowledgment. We thank the National Science Foundation for support of this research.

Supplementary Material Available: Tables of crystal data, positional parameters, bond distances and angles, and thermal parameters for compounds **5**, **8**, and **17–19** (55 pages). Ordering information is given on any current masthead page.

OM930212N